# Tests for observing $\nu_\tau$ interactions in a beam-dump experiment

Carl H. Albright

*Fermi National Accelerator Laboratory, Batavia, Illinois 60510*
*and Physics Department, Northern Illinois University, DeKalb, Illinois 60115*

Robert Shrock

*Physics Department, Princeton University, Princeton, New Jersey 08540*

J. Smith*

*CERN, Geneva 23, Switzerland*

(Received 18 June 1979)

We carry out a comparative analysis of three tests for the purpose of observing $\overset{(-)}{\nu}_\tau$ in a beam-dump experiment. The main source of $\overset{(-)}{\nu}_\tau$'s is determined to be the hadronic production of $F$ mesons, followed by the decay $F^\pm \to \tau^\pm \overset{(-)}{\nu}_\tau$. Possible signatures for various $\overset{(-)}{\nu}_\tau$-induced processes, together with their corresponding backgrounds, are examined. The muon-trigger test proposed earlier is found to be by far the most promising method. This test identifies $\overset{(-)}{\nu}_\tau$ events by the muonic decay mode of the $\tau^\pm$ produced in $\overset{(-)}{\nu}_\tau$ charged-current interactions, together with the requirements of substantial missing transverse momentum and distinctive behavior of certain azimuthal-angle distributions describing the emission of the muon, hadron shower, and direction of missing transverse momentum. It can be applied on an event-by-event basis, can separate $\nu_\tau$- and $\bar{\nu}_\tau$-induced reactions, and is specific to $\overset{(-)}{\nu}_\tau$. One should be able to use the test to determine directly whether $\nu_\tau$ is, indeed, a new, sequential neutrino. The test relies on the ability of recently developed neutrino detectors to measure the direction of the hadron shower. In addition to this muon-trigger test, we study the possibility of using two others, one based on the identification of events with two hadron showers, due to the semileptonic decay of the produced $\tau$, and the other based on the apparent neutral-to-charged-current event ratio. We find that neither of these two other tests seems feasible. However, it is expected that the muon-trigger test can be used in the near future to observe, for the first time, $\nu_\tau$ and $\bar{\nu}_\tau$.

## I. INTRODUCTION

The existence of the $\tau$ lepton has been well established in $e^+e^-$ experiments carried out at SPEAR[1,2] and at DORIS.[3] The most accurate measurement of its mass gave the value[2] $m_\tau = 1.782^{+0.002}_{-0.007}$ GeV. There are strong experimental and theoretical reasons for concluding that there exists a sequential neutrino, $\nu_\tau$, distinct from $\nu_e$ and $\nu_\mu$, associated with the $\tau$. However, so far, no experiment has definitely observed the interactions of a $\overset{(-)}{\nu}_\tau$ in matter. Recently, two of us proposed a test which could be used to make such an observation of $\overset{(-)}{\nu}_\tau$ in a beam-dump experiment.[4]

In this paper we shall discuss this test, which will be called the "muon-trigger test," in greater detail. Before proceeding to this discussion, which constitutes Sec. III, we shall analyze in Sec. II the sources, size, and characteristics of the $\overset{(-)}{\nu}_\tau$ flux in a beam-dump experiment, particularly in comparison with the $\overset{(-)}{\nu}_e$ and $\overset{(-)}{\nu}_\mu$ fluxes.

The reactions initiated by an incident $\overset{(-)}{\nu}_\tau$ include the neutral-current process

$$\overset{(-)}{\nu}_\tau + N \to \overset{(-)}{\nu}_\tau + X\,, \tag{1.1}$$

where $X$ denotes an arbitrary hadronic final state, and, given that the incident energy $E$ is greater than the threshold energy of 3.5 GeV, the charged-current processes

$$\overset{(-)}{\nu}_\tau + N \to \tau^\pm + X$$

$$\searrow \begin{cases} \overset{(-)}{\nu}_\tau + \text{hadrons} & (1.2) \\ \overset{(-)}{\nu}_\tau + e^\pm + \overset{(-)}{\nu}_e & (1.3) \\ \overset{(-)}{\nu}_\tau + \mu^\pm + \overset{(-)}{\nu}_\mu\,. & (1.4) \end{cases}$$

The question to be addressed is the following: Are there any distinctive characteristics of one or more of these reactions which can be used reliably to identify and isolate $\overset{(-)}{\nu}_\tau$ events from various backgrounds and thereby enable one justifiably to claim a definite observation of the $\tau$ neutrino? As was discussed in Ref. 4, we maintain that the reaction and decay chain (1.4) provides the best signal for $\overset{(-)}{\nu}_\tau$ events. Accordingly, the muon-trigger test was designed to utilize this process. The test, specifically, is to trigger on a single outgoing muon, apply standard cuts on the muon and hadron energies, search for missing transverse momentum, and, if it is found, test two azimuthal-angle correlations for certain distinctive features. A positive signal, we argue, would result only from process (1.4). The test has the merits that it can be used on an event-by-event basis and, furthermore, that it can separate the $\nu_\tau$- from the $\bar{\nu}_\tau$-induced version of process (1.4), thus making possible separate studies of spectral distributions for these two cases. At a theoretical level, the reaction and decay chain (1.3) is completely analogous to the process (1.4), with the obvious interchange of $e$ and $\mu$. However, it could not be used for our test because of experimental reasons: Conventional neutrino detectors cannot distinguish electrons from hadrons, and even in the most advanced detectors which have a reasonable capability of doing this there is still a significant probability of misidentifying the electron as part of the hadron shower. Moreover, the scattering angle and momentum of the scattered lepton can be measured more accurately for a muon than an electron. As will be explained below, the test allows for the possibility that there are more than three doublets of quarks and leptons; it is a specific test for $\nu_\tau$ and will not confuse it with additional sequential neutrinos, should they exist. Furthermore, it ought to be possible to use the test to check whether, indeed, it is true that the $\tau$ neutrino is a sequential neutrino, coupled to the $\tau$ in the manner specified by the usual doublet assignment in the now standard three-doublet Kobayashi-Maskawa version[5] of the Weinberg-Salam $SU(2)_L \times U(1)$ gauge theory.[6]

The muon-trigger test makes crucial use of the ability of a new, advanced generation of neutrino detectors which can measure not just the muon momentum, $\vec{p}_\mu$, the muon scattering angle, $\theta_\mu$, and the hadron energy deposition, $E_H$, but also the *direction* of the hadron shower. Such detectors can thus determine whether or not there is missing transverse momentum in a given event, to an accuracy which is expected[7] to be about $\pm 0.5$ GeV/$c$. The groups which are currently running or preparing neutrino experiments with beam-dump options and with this advanced type of detector, and that are therefore able to begin to apply our test include the CERN-Hamburg-Amsterdam-Rome-Moscow (CHARM),[8] Fermilab-MIT-MSU-NIU (FMMN),[9] and Michigan–Ohio State–Wisconsin (MOW)[10] collaborations. It is anticipated that other groups will soon be embarking on the development of similar sophisticated beam-dump experiments. From a purely empirical point of view, the existence of $\nu_\tau$ is currently an inference, albeit a strongly supported one, from $\tau$ decay data. An experiment which performs the muon-trigger test and finds a positive signal could claim to have observed directly, for the first time, a $\overset{(-)}{\nu}_\tau$. It would thus play a historic role analogous to the classic experiments[11,12] which first observed the interactions of free $\bar{\nu}_e$ and $\overset{(-)}{\nu}_\mu$ when their existence was still an inference from decay data.

Besides the muon-trigger test, there are two other tests which one might consider for the purpose of observing the $\nu_\tau$. The first of these involves the attempt to identify the two hadron showers which would result in events of type (1.2) where the $\tau$ decays semileptonically. The second tries to use the apparent neutral-to-charged-current event ratio as an indicator of the presence of a nonzero $\overset{(-)}{\nu}_\tau$ flux. Both are designed to be applied in beam-dump experiments. We shall examine these two other possible tests in Sec. IV and shall find that neither of them is as promising as the muon-trigger test, and, indeed, neither of them has much chance of success.

Before proceeding, it is useful to review first the evidence that $\nu_\tau$ is a sequential neutrino with the properties expected in the standard model.[5,6] Our treatment will be brief since the experimental data on $\tau$ and $\nu_\tau$ has been discussed in several recent reviews.[13] The existence of $\nu_\tau$ is inferred from a study of the momentum spectrum of $l=e$ or $\mu$ in leptonic $\tau$ decay, which is best described by the three-body mode $\tau^\pm \to \overset{(-)}{\nu}_\tau l^\pm \overset{(-)}{\nu}_l$. Within the framework of this inference, upper limits have been determined for the mass of the $\nu_\tau$; the best is $m(\nu_\tau) < 0.25$ GeV (at the 95% confidence level).[2,14] The momentum spectrum of $e$ or $\mu$ in the respective leptonic $\tau$ decay strongly favors a left-handed $\tau\nu_\tau$ vertex, with a weak coupling strength $g_{\tau\nu_\tau}{}^2 > 0.12 g_{l\nu_l}{}^2$, where $l=e$ or $\mu$.[2] Furthermore, from the relative rates of $e^+e^-$, $e^+\mu^- + e^-\mu^+$, and $\mu^+\mu^-$ events resulting from the reaction $e^+e^- \to \tau^+\tau^-$, one knows that $\tau^-$ cannot be an electron- or muon-type paralepton, i.e., it cannot have the lepton number of the $e^+$ or $\mu^+$. Hence $\nu_\tau \neq \bar{\nu}_e$ or $\bar{\nu}_\mu$. Moreover, from high-energy neutrino-scattering data one can conclude that $\nu_\tau \neq \overset{(-)}{\nu}_\mu$, since the process $\overset{(-)}{\nu}_\mu N \to \tau^\pm X$; $\tau^\pm \to e^\pm + \cdots$ is not observed.[15] So far, these data do not forbid the possibility that $\nu_\tau = \nu_e$. But in fact it is very hard and equally artificial to construct nonstandard gauge models in which $\nu_\tau = \nu_e$ without contradicting the experimental fact that, to within quoted error bounds,[1-3] $B(\tau \to eX) = B(\tau \to \mu X)$.

We next turn from direct experimental evidence to indirect theoretical arguments concerning the properties of $\nu_\tau$. These are based on the fact that the standard three-doublet Kobayashi-Maskawa version[5] of the Weinberg-Salam model,[6] with the generalized Glashow-Iliopoulos-Maiani mechanism[16] incorporated, is at present the most successful theory in its ability to account for the known fermions and in its confrontation with data on weak decays and charged- and neutral-current reactions.[17] In this model the requirement of the absence of tree-level strangeness-changing neutral currents, and its extension, via the principle of quark-lepton universality, to natural flavor conservation by the neutral current, implies that all fermions of a given charge and chirality must have the same weak $T$ and $T_3$.[18] For leptons this is also implied by the requirement of natural suppression of $\mu$- and $e$-number nonconservation, should it exist at all.[19] Hence, given the SU(2) doublet assignments for the left-handed components of the two old families of leptons, the $\tau$ must also be placed in a doublet $\binom{\nu_\tau}{\tau}_L$. This is independently required by anomaly cancellation, given the analogous assignment of the $\Upsilon$-constituent quark $b$ to a doublet $\binom{t}{b}_L$ (which, of course, presupposes the existence of a $t$ quark). Based on these experimental and theoretical grounds, we consider it reasonably well, although partially indirectly, established that $\nu_\tau$ is a sequential neutrino which couples to $\tau$ in the same way that $\nu_l$ couples to $l$, where $l=e$ or $\mu$. Part of the appeal of the muon-trigger test to be described in Sec. III is that it should provide a direct experimental check of this conclusion regarding $\nu_\tau$. We proceed to analyze the (anti)neutrino fluxes in a beam-dump experiment.

## II. NEUTRINO FLUXES IN A BEAM-DUMP EXPERIMENT

In order to study the feasibility of a test for $\overset{(-)}{\nu}_\tau$'s in a beam-dump experiment, it is necessary to have at least an approximate calculation of the expected flux of $\overset{(-)}{\nu}_\tau$'s and, in addition, $\overset{(-)}{\nu}_\mu$'s and $\overset{(-)}{\nu}_e$'s. A beam dump is used in order to enhance the flux of $\overset{(-)}{\nu}_\tau$'s relative to that of the latter two types of neutrinos, which produce the main physics backgrounds to a test for $\overset{(-)}{\nu}_\tau$'s. This enhancement is a consequence of the fundamental characteristic of a beam dump: The proton beam is incident on a thick target-absorber composed of a material with high atomic number $A$. Thus, $\pi$'s and $K$'s produced in the initial proton-nucleus collisions are absorbed before they have a chance to decay weakly, yielding neutrinos. This suppresses the $\overset{(-)}{\nu}_\mu$ flux (from $\pi_{\mu 2}$, $K_{\mu 2}$, and, to a lesser extent, $K_{\mu 3}$ decays) and the $\overset{(-)}{\nu}_e$ flux (from $K_{e3}$ decays) by a factor which depends on the type of beam dump, but is generally of order several hundred. In contrast, hadrons composed of heavy quarks with very short lifetimes do decay, so that, to the extent that the absorption of $\pi$'s and $K$'s is complete, the neutrino flux emerging from the beam dump has a composition determined by the weak decays of the short-lived heavy hadrons. The only heavy hadrons produced in significant numbers are those containing charmed quarks; of these the pseudoscalar mesons $D$ and $F$ constitute the dominant source of neutrinos, which result from their leptonic and semileptonic decays. Thus, denoting the flux of $\overset{(-)}{\nu}_l$'s as $N(\overset{(-)}{\nu}_l)$, where $l=e$, $\mu$, or $\tau$, $N(\nu_e)\simeq N(\bar\nu_e)\simeq N(\bar\nu_\mu)\lesssim N(\nu_\mu)$. Furthermore, $N(\nu_\tau)\simeq N(\bar\nu_\tau)$, which would hold as an equality if the only associated-charm-production reactions were of the form $pN\to(M_c\overline{M}_cX, B_c\overline{B}_cX)$, where $M_c$ and $B_c$ denote a genuine charmed meson and baryon, respectively (and $X$ represents an arbitrary hadronic final state not containing charmed particles). The presence of production modes such as $pN\to(M_c\overline{B}_cX, \overline{M}_cB_cX)$ causes a difference in the $\nu_\tau$ versus $\bar\nu_\tau$ yield, which, however, is sufficiently small to be negligible for our purposes.

There are several interrelated questions concerning the $\overset{(-)}{\nu}_\tau$ flux: First, what are the main sources of such neutrinos; second, how large is $N(\overset{(-)}{\nu}_\tau)$ relative to $N(\overset{(-)}{\nu}_l)$, where $l=e$ or $\mu$; and third, what is the absolute magnitude and energy dependence of $N(\overset{(-)}{\nu}_l)$, $l=e$, $\mu$, or $\tau$. In Ref. 4 the first question was answered and an approximate estimate was given for the second. Let us review the details of these results. The main source of $\overset{(-)}{\nu}_\tau$'s was determined to be the associated production of $F\overline{F}$ pairs (taken to include strong production and decay chains such as $pN\to F^\pm F^{*\mp}X$; $F^{*\pm}\to F^\pm\gamma$, etc.), followed by the leptonic decay $F^\pm\to\tau^\pm\overset{(-)}{\nu}_\tau$. This finding contradicts the recent analysis by Barger and Phillips,[20] who neglected the decay $F^\pm\to\tau^\pm\overset{(-)}{\nu}_\tau$ and stated that the $\overset{(-)}{\nu}_\tau$ flux would arise mainly from the hadronic production and (semi)leptonic decays of heavy $b$- and $t$-flavored particles. In fact, as will be seen below, $b$- and $t$-flavored hadrons yield a $\overset{(-)}{\nu}_\tau$ flux which is completely negligible compared to that from the $F\overline{F}$ source.

The $\overset{(-)}{\nu}_\tau$ production rate due to $F\overline{F}$ production and leptonic decay is determined by the quantity $\sigma(pN\to F^+F^-X)B(F^\pm\to\tau^\pm\overset{(-)}{\nu}_\tau)$. For the $F^+F^-$ hadronic production cross section at a typical incident proton energy of 400 GeV we use the conservative estimate[21]

$$\begin{aligned}\sigma(pN\to F\overline{F}X) &\simeq \left(\frac{\sigma(pN\to K\overline{K}X)}{\sigma(pN\to\pi\pi X)}\right)\sigma(pN\to D\overline{D}X)\\ &\simeq 0.1\sigma(pN\to D\overline{D}X)\,.\end{aligned}\tag{2.1}$$

The ratio of $\pi$ to $\overset{(-)}{K}$ production cross sections is supposed to incorporate the effect of having to produce an $\bar{s}s$ pair for inclusion in the $F^+$ and $F^-$ mesons. However, the use of this factor could easily represent an underestimate of $\sigma(pN\to F^+F^-X)$, since $m_\pi^2/m_K^2$ is significantly smaller than $m_D^2/m_F^2$, reflecting the fact that of all of the pseudoscalar mesons, the pion is by far the closest to being an almost Goldstone boson, thus the lightest, and hence in general the easiest to produce. The (forward angle part of the) hadronic charm production cross section has been measured, via the event rate for regular neutrinos, in recent CERN and Caltech-Fermilab beam-dump experiments.[22] The results of these experiments indicate that this cross section is ~50–100 $\mu$b. It would be valuable to have further data on the hadronic production cross sections for $D\bar{D}$ and especially $F\bar{F}$.

The branching ratio for the decay $F^\pm \to \tau \overset{(-)}{\nu}_\tau$ is

$$B(F^+ \to \tau^+\nu_\tau) = \frac{\Gamma(F^+ \to \tau^+\nu_\tau)}{\Gamma(F \to \text{all})}\,, \tag{2.2a}$$

where

$$\Gamma(F^+ \to \tau^+\nu_\tau) = \frac{G_F{}^2 |V_{cs}|^2 m_\tau{}^2 f_F{}^2 m_F}{8\pi}\left(1 - \frac{m_\tau{}^2}{m_F{}^2}\right)^2 \tag{2.2b}$$

and

$$\Gamma(F^+ \to \text{all}) \simeq \frac{G_F{}^2(|V_{cd}|^2 + |V_{cs}|^2) m_c{}^5}{192\pi^3}\,(2 + 3\lambda)\,. \tag{2.2c}$$

In Eq. (2.2b) $V_{ij}$ denotes the element of the quark mixing matrix $V$ which modulates the weak transition between $q_i$ and $q_j$. From a recent analysis of bounds on quark mixing angles in the standard six-quark model,[23,24] we have $|V_{cs}| \sim 0.85$–$0.95$ and $|V_{cd}| \sim 0.20$–$0.22$. The quantity $f_F$ denotes the pseudoscalar decay constant for leptonic $F$ decay, which was conservatively taken to be equal to $f_K$ in Ref. 4 but could be somewhat larger.[25] Equation (2.2c) is the usual quark-model expression for the charm decay rate; $\lambda$ represents the nonleptonic enhancement factor and is taken to be $\lambda \simeq 2.7$, as determined roughly by the measured semileptonic branching ratio $B(D \to eX) \simeq 0.1$.[26] The mass of the $F$ has been measured by the DASP collaboration[27] to be $m_F = 2.03 \pm 0.06$ GeV. The SLAC-LBL experiment[27] has also reported a tentative $F$ signal, with $m_F = 2.0395 \pm 0.001$ GeV. Using the latter value and combining it with the other inputs, we obtain $B(F^+ \to \tau^+\nu_\tau) \simeq 0.03$. This branching ratio may then be combined with Eq. (2.1) to yield an approximate total rate for $\overset{(-)}{\nu}_\tau$ production via hadronic $F\bar{F}$ production and leptonic decay.[28]

In addition to this source of $\overset{(-)}{\nu}_\tau$'s, one might consider three others: (1) hadronic production of $D^+D^-$ pairs, followed by the leptonic decay $D^\pm \to \tau^\pm \overset{(-)}{\nu}_\tau$; (2) hadronic production of heavy pseudoscalar mesons $M \equiv M(b\bar{u})$ followed by the corresponding leptonic decay $M^\pm \to \tau^\pm \overset{(-)}{\nu}_\tau$; and (3) the Drell-Yan process $pN \to \tau^+\tau^- X$; $\tau^\pm \to \nu_\tau X'$. We analyze these in turn. The rate for $\overset{(-)}{\nu}_\tau$ production via the $D^+D^-$ charmed decay, relative to that via the corresponding $F^+F^-$ channel, is

$$\frac{R(pN \to D^+D^-X \to \nu_\tau \overset{(-)}{\nu}_\tau X')}{R(pN \to F^+F^-X \to \nu_\tau \overset{(-)}{\nu}_\tau X')} = \frac{\sigma(pN \to D^+D^-X)}{\sigma(pN \to F^+F^-X)}\,\frac{B(D^\pm \to \tau^\pm \overset{(-)}{\nu}_\tau)}{B(F^\pm \to \tau^\pm \overset{(-)}{\nu}_\tau)} \simeq 0.1\,, \tag{2.3}$$

where we have used the fact that for typical allowed values of quark mixing angles and $f_D = f_K$, the branching ratio $B(D^\pm \to \tau^\pm \overset{(-)}{\nu}_\tau) \simeq (1-3)\times 10^{-4}$. Thus, the larger hadronic cross section for production of a $D^+D^-$, as opposed to an $F^+F^-$ pair is more than offset, first by the mixing-angle suppression, and secondly, by the phase-space suppression, of the $D^\pm \to \tau^\pm \overset{(-)}{\nu}_\tau$ decay mode. One may then anticipate that this source will augment the $\overset{(-)}{\nu}_\tau$ yield from hadronic $F\bar{F}$ production and leptonic decay by about 10%. We have conservatively neglected this additional contribution in our estimate of the $\overset{(-)}{\nu}_\tau$ flux.

It is easy to show that the second possible additional source of $\overset{(-)}{\nu}_\tau$'s, viz. hadronic associated production of pseudoscalar mesons $M \equiv M(b\bar{u})$ which then decay leptonically to $\tau^-\bar{\nu}_\tau$, is negligible. Proceeding along the same lines as before, we first use a standard scaling relation[29] to estimate the hadronic production cross section for the $M$ mesons:

$$\sigma(pN \to M\bar{M}X) \simeq \left(\frac{\sigma(pN \to \Upsilon X)}{\sigma(pN \to \psi X)}\right)\sigma(pN \to D\bar{D}X) \simeq 10^{-4}\sigma(pN \to D\bar{D}X)\,. \tag{2.4}$$

The branching ratio for the decay $M^\pm \to \tau^\pm \overset{(-)}{\nu}_\tau$ can be calculated as in Eqs. (2.2a)–(2.2c) with the replacement in Eq. (2.2b) of $m_F$ by $m_M \simeq 5$ GeV, $f_F$ by $f_M$, and $V_{cs}$ by $V_{ub}$. Various estimates[25] give $f_M \sim 0.5$ GeV. From a recent generalized Cabibbo fit[23] and subsequent complete determination of bounds on quark mixing angles in the standard six-quark model we know that[24] $|V_{ub}| = 0.06^{+0.06}_{-\Delta}$ where the lower error bound is such that $|V_{ub}|_{\text{min}} \sim 10^{-4}$. Further, in Ref. 24 the decay rate of the $b$ quark was calculated; this result can be used here, assuming the reasonable relation $\Gamma_M \simeq \Gamma_b$. Typical values were $\Gamma_b = \hbar/\tau_b$, where $\tau_b \simeq (2-7) \times 10^{-14}$ sec. Combining the central values of these inputs, we find that $B(M^+ \to \tau^+\nu_\tau) \sim 4 \times 10^{-3}$; rough extremal values of this branching ratio, obtained by using minimum- or maximum-allowed values of the inputs, are $\sim 10^{-9} \lesssim B(M^+ \to \tau^+\nu_\tau) \lesssim 0.03$. Hence the production rate of $\overset{(-)}{\nu}_\tau$'s from this source, relative to that from $F\bar{F}$ pairs, is

$$\frac{R(pN \to M^+M^-X \to \nu_\tau \overset{(-)}{\nu}_\tau X')}{R(pN \to F^+F^-X \to \nu_\tau \overset{(-)}{\nu}_\tau X')} \lesssim 10^{-3}\,, \tag{2.5}$$

with the central value being ~$10^{-4}$ and an estimated minimal value being $\sim 10^{-9}$. Thus, far from being the dominant source of $\overset{(-)}{\nu}_\tau$'s, as was assumed in Ref. 20, this is a negligible source. The same conclusion applies, *a fortiori,* to the $\overset{(-)}{\nu}_\tau$ flux from the production and decay of hadrons containing still heavier quarks, such as $t$.

Finally, we consider Drell-Yan production[30] of $\tau^+\tau^-$ pairs. The cross section for this process is bounded above by that for $\mu^+\mu^-$ and $e^+e^-$ Drell-Yan production, which has been well measured from dilepton invariant masses $m_{l^+l^-}$ in the vector-meson resonance region out to $m_{l^+l^-} \simeq 14$ GeV (and agrees nicely with the theoretical prediction away from regions where the latter is inapplicable, i.e., masses of vector mesons).[31] From a previous calculation of the total cross section for Drell-Yan production of charged heavy lepton pairs we have[32] $\sigma(pp\to\tau^+\tau^-X)\sim 4\times 10^{-34}$ cm$^2$, which is smaller by about a factor of $10^3$ than the product of cross section times branching ratio for the dominant $F\overline{F}$ source of $\overset{(-)}{\nu}_\tau$. Indeed, the above number is an overestimate of the Drell-Yan contribution, since only the forward angle part of the cross section is relevant here.

Having determined the main source of $\overset{(-)}{\nu}_\tau$'s, one may next investigate the size of the $\overset{(-)}{\nu}_\tau$ flux relative to that of $\overset{(-)}{\nu}_e$'s and $\overset{(-)}{\nu}_\mu$'s. In Ref. 4 a rough estimate for this ratio was given, for an ideal beam dump in which $\pi$'s and $K$'s are completely absorbed. In this case all types of (anti)-neutrinos arise from the decays of charmed hadrons (presumably mainly charmed mesons) produced in the initial $pN$ collisions. Consequently, the somewhat uncertain absolute charm production cross section cancels in the ratio, and one has

$$\frac{N(\overset{(-)}{\nu}_\tau)}{N(\overset{(-)}{\nu}_l)} \simeq \frac{\sigma(pN\to F^+F^-X)}{\sigma(pN\to D^+D^-X)}\,\frac{2B(F^\pm\to\tau^\pm\overset{(-)}{\nu}_\tau)}{B(D^\pm\to l^\pm\overset{(-)}{\nu}_l X)}$$

$$\simeq 0.06\,, \qquad (2.6)$$

where $l=e$ or $\mu$. The numerator of Eq. (2.6) will be slightly increased by the $D^\pm\to\tau^\pm\overset{(-)}{\nu}_\tau$ contribution, while the denominator will be augmented slightly by the production and semileptonic decay of charmed baryons; in the spirit of this rough estimate both effects are neglected. The factor of 2 in the numerator is included because the decay of the $\tau^\pm$ yields an additional direct $\overset{(-)}{\nu}_\tau$. In contrast, in the denominator, even if $l=\mu$, for any relevant laboratory energy (greater than $\sim 0.1$ GeV) the $\mu$ would not decay before passing the detector. Substituting the value of $B(F^\pm\to\tau^\pm\overset{(-)}{\nu}_\tau)$ calculated in Eq. (2.2) and the measured branching ratio $B(D^\pm\to e^\pm X)\simeq 0.1$ yields the number given in Eq. (2.6). It was remarked[4] that this estimate should be accurate to within factors of a few. The main corrections to it include: (1) for beam-dump materials of lower $A$, the incomplete absorption of $\pi$'s and $K$'s, which increase the $\overset{(-)}{\nu}_e$ and $\overset{(-)}{\nu}_\mu$ fluxes; (2) the effect of $D^\pm\to\tau^\pm\overset{(-)}{\nu}_\tau$ and semileptonic charmed-baryon decay, as noted above; (3) the slightly different dependence of the invariant differential cross sections for the hadronic production of $F\overline{F}$ versus $D\overline{D}$ on the variables $x_F\equiv p_\parallel/(p_\parallel)_{\max}$ and $p_T$ of the respective mesons; (4) the differences in the laboratory angular distribution of, and hence detector acceptance for, the $\overset{(-)}{\nu}_{e,\mu}$ from $D$ decay, the initial $\overset{(-)}{\nu}_\tau$, denoted $\nu_{\tau 1}$, from leptonic $F$ decay, and the second $\overset{(-)}{\nu}_\tau$, denoted $\overset{(-)}{\nu}_{\tau 2}$, from the subsequent decay of the $\tau$. Moreover, Eq. (2.6) makes no reference to the different energy dependences of the various (anti)neutrino spectra.

It would be inappropriate here to carry out a full calculation of the spectra $N(\overset{(-)}{\nu}_l; E)$, $l=e$, $\mu$, and $\tau$, since this would depend on the detailed geometry of each particular beam-dump apparatus. However, certain general characteristics of the flux spectra are evident. To the extent that the flux of $\overset{(-)}{\nu}_e$'s and $\overset{(-)}{\nu}_\mu$'s arises mainly from semileptonic $D$ decays, in the rest frame of the parent $D$, $\langle|\vec{p}(\overset{(-)}{\nu}_l)_D|\rangle\sim 0.3m_D$, where the subscript $D$ indicates the reference frame; the greater the hadron multiplicity, the smaller $\langle|\vec{p}(\overset{(-)}{\nu}_l)|\rangle$ is. In contrast, the $\overset{(-)}{\nu}_\tau$'s come from two quite different kinds of decays. The $\overset{(-)}{\nu}_{\tau 1}$ has a definite and small three-momentum in the $F$ rest frame; $|\vec{p}(\overset{(-)}{\nu}_{\tau 1})_F|=0.24$ GeV. For the second, $|\langle\vec{p}(\overset{(-)}{\nu}_{\tau 2})_\tau\rangle|\sim 0.3m_\tau\sim 0.5$ GeV, depending on the specific decay mode of the $\tau$. Although the angular dependences for neutrino emission in these two decay processes are different, to the extent that both $\overset{(-)}{\nu}_{\tau 1}$ and $\overset{(-)}{\nu}_{\tau 2}$ are emitted at angles such that in the laboratory frame they travel toward the detector (which, of course, is the only case relevant here), $\overset{(-)}{\nu}_{\tau 2}$ will generally have substantially higher laboratory energy than $\overset{(-)}{\nu}_{\tau 1}$. This two-component nature of the $\overset{(-)}{\nu}_\tau$ flux will be evident in the curves to be presented shortly.

Another general feature of the (anti)neutrino flux from $D$ and $F$ decay is that, because of the large masses of such charmed hadrons, it extends farther out in $p_T$ than the $\overset{(-)}{\nu}_\mu$ and $\overset{(-)}{\nu}_e$ flux from $\pi$ and $K$ decay. Accordingly, one method of further suppressing the $\overset{(-)}{\nu}_l$ flux from $\pi$ and $K$ decay and thereby indirectly increasing the ratio $N(\overset{(-)}{\nu}_\tau)/N(\nu_l)$, $l=e$ or $\mu$, is to mis-steer the beam slightly so that the detector is not directly in line with the beam, and hence it samples a $\theta_{\text{lab}}\neq 0$, $p_T\neq 0$ part of the neutrino flux.

Previous calculations of neutrino fluxes from $\pi$ and $K$ decays have been tabulated by Stefanski and White.[33] Using parametrizations of hadronic production cross sections,[34] Mori[35] has performed a

Monte Carlo calculation of neutrino fluxes from a typical beam-dump experiment. The fluxes apply for the case in which a 400 GeV proton beam is incident on a beam dump made of copper, and the detector is located 250 m downstream from the dump. The angular region subtended by the fiducial volume of the detector is taken conservatively to be 0–2 mrad. The results are presented in Fig. 1. Curves labeled $\overset{(-)}{\nu}_l$ represent the $\nu_l$ or $\bar{\nu}_l$ flux from a source which yields equal numbers of $\nu_l$ and $\bar{\nu}_l$. Note that $\overset{(-)}{\nu}_e$ (total)$\simeq\overset{(-)}{\nu}_e(D)$. The $\overset{(-)}{\nu}_\tau$ fluxes are computed assuming that

$$E\frac{\partial^3\sigma}{\partial p^3}\,(pN\to\overset{(-)}{F}X)=\frac{Ag(p_T,s)G(x_F)}{[(p_T^{\,2}+m_F^{\,2})^{1/2}+2.7]^{16.5}}\,,\tag{2.7a}$$

where

$$g(p_T,s)=\begin{cases}\exp(-1.06p_T), & p_T\le 1.0\\ \exp[(1-p_T)s^{-1/2}-1.06], & p_T\ge 1.0\,.\end{cases}\tag{2.7b}$$

$$G(x_F)=\begin{cases}1, & |x_F|\le 0.25\\ \left(\dfrac{1-|x_F|}{0.75}\right)^4, & |x_F|\ge 0.25\,.\end{cases}\tag{2.7c}$$

with $p_T$, $m_F$, and the center-of-mass energy $\sqrt{s}$ expressed in units of GeV. The ratio $\sigma(pN\to\overset{(-)}{F}X)=0.1\sigma(pN\to\overset{(-)}{D}X)$ is used from Ref. 4, and the constant $A$ is then determined such that the differential cross section for associated $D$ production, integrated from $(\theta_D)_{\rm lab}=0$ to 200 mrad, is equal to 100 $\mu$b. Further, the value $B(F^+\to\tau^+\nu_\tau)$ is taken from Ref. 4. The $\tau$ decay modes which were included are $\tau^-\to\nu_\tau l\bar{\nu}_l$ with $l=e$ or $\mu$, each with a branching ratio of 0.19, together with the two two-body semileptonic modes $\tau^-\to\nu_\tau\pi^-$ and $\tau^-\to\nu_\tau\rho^-$, with branching ratios of 0.1 and 0.2. Higher multiplicity decay modes are not included because of the lack of knowledge concerning the form of the differential decay distributions for these modes. Since only 68% of the $\tau$ decay modes are included, the resulting $\overset{(-)}{\nu}_\tau$ curves are underestimates and should be multiplied by roughly $(0.68)^{-1}\simeq1.5$ to obtain the true $\overset{(-)}{\nu}_\tau$ flux. Actually one anticipates that since the average three-momentum of $\nu_{\tau 2}$ in the $\tau$ rest frame decreases as the multiplicity of the decay mode increases, the additional modes will tend to populate preferentially the lower-energy part of the $\overset{(-)}{\nu}_\tau$ spectrum. The two-component nature of the $\overset{(-)}{\nu}_\tau$ flux is evident in Fig. 1; there is a peak in $N(\overset{(-)}{\nu}_\tau)$ at $E\sim25$–30 GeV and a marked high-energy shoulder in the region from 100 to 150 GeV. The incomplete suppression of $\overset{(-)}{\nu}_\mu$'s and $\overset{(-)}{\nu}_e$'s from $\pi$ and $K$ decay can also be seen

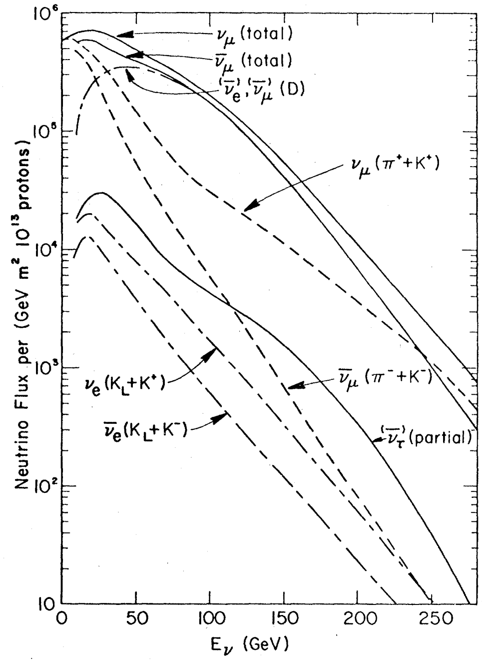


FIG. 1. Neutrino and antineutrino fluxes for a detector subtending an angular region of 0 to 2 mrad, located 250 m downstream from a copper beam dump on which 400-GeV protons are incident. Curves are from calculations by Mori (Ref. 35).

in the figure. If one were to use a beam-dump material of higher $A$ than that of copper, such as tungsten, this suppression would be more effective. Multiplying the $\overset{(-)}{\nu}_\tau$ fluxes by 1.5 and comparing $N(\overset{(-)}{\nu}_\tau)/N(\overset{(-)}{\nu}_l)$ as a function of energy to our crude overall estimate of 0.06 for an ideal beam dump, one finds reasonable agreement. For example, for the set of values $E=(25,50,100,150)$ GeV, the ratio $N(\overset{(-)}{\nu}_\tau)/N(\nu_\mu)$ takes the corresponding set of values $(0.06,0.05,0.03,0.03)$, while $N(\overset{(-)}{\nu}_\tau)/N(\overset{(-)}{\nu}_e)=(0.14,0.07,0.04,0.04)$. For further details concerning the calculation of the fluxes of Fig. 1 the reader should consult Ref. 35.

In addition to this analysis a valuable computation of the $\overset{(-)}{\nu}_e$ and $\overset{(-)}{\nu}_\mu$ (but not $\overset{(-)}{\nu}_\tau$) fluxes from three different kinds of beam dumps, composed of Be, Cu, and W, has been carried out for the MOW experiment[10] by Roe.[36] Neutrino flux calculations have also been performed for the analysis of the data from previous beam-dump experiments using bubble chambers and conventional electronic neutrino detectors.[22]

Having discussed the sources and characteristics of the (anti)neutrino fluxes in a typical beam-dump experiment and specified in Fig. 1 the fluxes which will be used for our work, we next proceed to describe the tests for $\overset{(-)}{\nu}_\tau$.

## III. THE MUON-TRIGGER TEST

The method which appears to be the most promising one for observing $\overset{(-)}{\nu}_\tau$, as proposed in Ref. 4 is to trigger on an outgoing muon and test for substantial missing transverse momentum and certain distinctive azimuthal-angle correlations. Here we shall elaborate on the details of this test.

As described in the previous section, the $\overset{(-)}{\nu}_\tau$'s originate predominantly from the decays of $F$ mesons produced in the initial proton-nucleus collisions. A beam dump is used because it enhances the $\overset{(-)}{\nu}_\tau$ flux relative to the $\overset{(-)}{\nu}_\mu$ and $\overset{(-)}{\nu}_e$ fluxes, which produce the main physics backgrounds (as opposed to the background due to imperfect accuracy in the measurement of $\vec{p}_H$ and $\vec{p}_\mu$).

The test is based on the following fundamental property of $\nu_\tau$: it couples via the usual charged current to $\tau$, which is short-lived and hence will certainly decay within the detector (indeed, typically within ~1 cm of its production vertex). By requiring an outgoing muon, one selects events due to the reaction and decay chain (1.4): $\overset{(-)}{\nu}_\tau N \to \tau^\pm X$; $\tau^\pm \to \nu_\tau \mu^\pm \overset{(-)}{\nu}_\mu$, so that there are two missing neutrinos. As was expected and was verifed by Monte Carlo calculations,[4] in general these two neutrinos carry off substantial momentum tranverse to the (experimentally known) incident $\overset{(-)}{\nu}_\tau$ direction, $\hat{n}_b$. This is schematically illustrated in Figs. 2(a) and 2(b). The test, then, consists of the following steps: (1) trigger on a single outgoing muon; (2) apply the standard cuts used in counter neutrino experiments, on $E'$ (the scattered muon energy), $E_H$ (the hadronic deposition), and optionally, $\theta_\mu$ (the muon scattering angle); and (3) from $\hat{n}_b$ and the measured muon and hadron spray momenta $\vec{p}_\mu$ and $\vec{p}_H \equiv E_H \hat{p}_H$[37] test to determine if, within the accuracy of the experiment, (a) $(\vec{p}_\perp)_{\text{missing}}$ is nonzero, where

$$(\vec{p}_\perp)_{\text{missing}} \equiv -(\vec{p}_\mu + \vec{p}_H)_\perp \,, \tag{3.1}$$

with

$$\vec{p}_\perp \equiv \vec{p} - (\vec{p}\cdot\hat{n}_b)\hat{n}_b \,, \tag{3.2}$$

i.e., there is missing momentum transverse to the beam direction, and/or (b) $(\vec{p}_T)_{\text{missing}}$ is nonzero, where

$$(\vec{p}_T)_{\text{missing}} \equiv -(\vec{p}_\mu + \vec{p}_H)_T \,, \tag{3.3}$$

$$\vec{p}_T \equiv (\vec{p}\cdot\hat{n}_{pp})\hat{n}_{pp} \,, \tag{3.4}$$

and

$$\hat{n}_{pp} \equiv \frac{\hat{n}_b \times \hat{p}_\mu}{|\hat{n}_b \times \hat{p}_\mu|} \tag{3.5}$$

is the normal to the apparent production plane. In the $\overset{(-)}{\nu}_\tau$-induced process (1.4) which is selected by the trigger, $(\vec{p}_i)_{\text{missing}}$ will of course be equal to $[\vec{p}(\overset{(-)}{\nu}_\tau) + \vec{p}(\overset{(-)}{\nu}_\mu)]_i$, where $i = \perp$ or $T$. For events in which there is significant missing transverse momentum, two further key diagnostic quantities to analyze are the (independent) azimuthal angles

$$\Delta\varphi_{\mu H} \equiv \sin^{-1}|(\hat{p}_\mu)_\perp \times (\hat{p}_H)_\perp| \tag{3.6}$$

and

$$\Delta\varphi_{mH} \equiv \sin^{-1}|(\hat{p}_\perp)_{\text{missing}} \times (\hat{p}_H)_\perp| \tag{3.7}$$

(where "$m$" stands for "missing"). For reaction (1.4) $\Delta\phi_{mH}$ is the azimuthal angle between $[\vec{p}(\overset{(-)}{\nu}_\tau) + \vec{p}(\overset{(-)}{\nu}_\mu)]_\perp$ and $(\vec{p}_H)_\perp$. As will be explained later, the last part of the test is (4) to examine whether (a) $\Delta\phi_{\mu H} > 90°$ and (b) $\Delta\phi_{mH} > 120°$. It is our claim that steps (1) through (4) constitute a feasible test for observing $\tau$ (anti)neutrinos. An obvious but important feature of the test is that since the sign of the outgoing muon tags the event as having been initiated by an incident $\nu_\tau$ or $\bar{\nu}_\tau$, it is possible to study separately the characteristics of $\nu_\tau$ versus $\bar{\nu}_\tau$ charged-current reactions. Furthermore, the test is specific to $\overset{(-)}{\nu}_\tau$ and would not confuse it with other additional sequential neutrinos, even if they exist. One may also be able to use it to check whether the data are consistent with the usual sequential assignment for $\overset{(-)}{\nu}_\tau$. Both of these features will be discussed further below.

Until the present time no counter experiment would have been able to perform this test, since none was able to measure with reasonable accuracy the direction of $\hat{p}_H$ of the hadron spray. However, the new CHARM,[8] FMMN,[9] and MOW[10] experiments have detectors which do have some capability to carry out such a measurement. The degree of

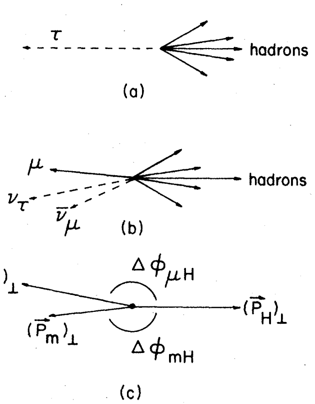


FIG. 2. Schematic illustration showing the view along the beam direction of (a) the initial scattering process $\nu_\tau N \to \tau + \text{hadrons}$; and (b) the process after the decay $\tau \to \nu_\tau \mu \bar{\nu}_\mu$ (where dashed lines indicate unobserved particles); together with (c) the definitions of the azimuthal angles $\Delta\phi_{\mu H}$ and $\Delta\phi_{mH}$.

success with which these experiments can perform our test depends on the accuracy with which they can measure $\vec{p}_H$ and hence test for missing transverse momentum. Estimates indicate[7] that it will be possible to measure $(p_\perp)_{\text{missing}}$ to an accuracy of ~±0.5 GeV/$c$, which should be sufficient by our test. Although all of these experiments are multipurpose, they intend to spend a significant portion of their running time in the beam-dump mode. It may be hoped, therefore, that this test can feasibly be performed in the near future.

We have carried out a Monte Carlo calculation as reported in Ref. 4, of the production and decay sequence (1.4): $\overset{(-)}{\nu}_\tau N \to \tau^\pm X$; $\tau^\pm \to \overset{(-)}{\nu}_\tau \mu^\pm \overset{(-)}{\nu}_\mu$. The differential cross section for the production of a $\tau$ with spin $s_\mu$ is

$$\frac{\partial^2\sigma}{\partial x \partial y}[\overset{(-)}{\nu}_\tau(l_1)+N(p)\to\tau^\pm(l_2;s)+X]=\frac{G_F{}^2 m_N E}{\pi}(T_0+T_s)\,, \tag{3.8}$$

where the spin-independent and spin-dependent terms are respectively

$$T_0=y(xy+\delta_\tau)F_1+[1-y-\delta_N(xy+\delta_\tau)]F_2\pm y[x(1-\tfrac{1}{2}y)-\tfrac{1}{2}\delta_\tau]F_3+\delta_\tau(xy+\delta_\tau)F_4-\delta_\tau F_5\,, \tag{3.9}$$

and

$$T_s=-\left(\frac{m_\tau}{m_N E}\right)\{ys\cdot l_1F_1+(s\cdot p-\delta_N s\cdot l_1)F_2\mp\tfrac{1}{2}[s\cdot q+(xy+\delta_\tau)s\cdot p]F_3+[-2(xy+\delta_\tau)s\cdot q+xys\cdot l_1]F_4$$
$$+\tfrac{1}{2}[-(xy+\delta_\tau)s\cdot p+s\cdot q-ys\cdot l_1]F_5\}\,. \tag{3.10}$$

In Eqs. (3.8)–(3.10) $E$ and $E'$ denote the incident-$\overset{(-)}{\nu}_\tau$ and scattered-$\tau^\pm$ laboratory energies, $q=(l_1-l_2)$, $x=Q^2/(2m_N\nu)$, $y=\nu/E$, $Q^2=-q^2$, $\nu=p\cdot q/m_N=(E-E')$, $\delta_i=m_i{}^2/(2m_NE)$ with $i=N$ or $\tau$, and the $\pm$ sign applies for incident $\nu_\tau$ and $\bar\nu_\tau$, respectively. The structure functions $F_i$ are defined by the standard expression for the hadron tensor,

$$W_{\mu\nu}(p,q)=-g_{\mu\nu}W_1+\frac{p_\mu p_\nu}{m_N{}^2}W_2-\frac{i\epsilon_{\mu\nu\alpha\beta}p^\alpha q^\beta}{2m_N{}^2}W_3+\frac{q_\mu q_\nu}{m_N{}^2}W_4+\frac{1}{2m_N{}^2}(p_\mu q_\nu+q_\mu p_\nu)W_5 \tag{3.11}$$

together with the scaling relations $m_NW_1(\nu,q^2)\to F_1(x)$ and $\nu W_i(\nu,q^2)\to F_i(x)$, $i=2,\ldots,5$, valid in the Bjorken limit. The kinematically allowed region for the production reaction is specified by

$$\frac{\delta_\tau}{(1-m_\tau/E)}\leq x\leq 1 \tag{3.12}$$

and

$$A-B\leq y\leq A+B\,, \tag{3.13a}$$

where

$$A=\frac{1}{2}\left[1-\delta_\tau\left(\frac{1}{x}+2\delta_N\right)\right]\Big/(1+x\delta_N) \tag{3.13b}$$

and

$$B=\frac{1}{2}\left[\left(1-\frac{\delta_\tau}{x}\right)^2-\frac{m_\tau{}^2}{E^2}\right]^{1/2}\Big/(1+x\delta_N)\,. \tag{3.13c}$$

Because of the left-handed leptonic scattering vertex, for $E$ and $E'$ sufficiently large that $m_\tau/E'\ll 1$, the $\tau^\pm$ is produced with strong longitudinal polarization (helicity) $P_L(\tau^\pm)=\pm1+O(m_\tau{}^2/E'^2)$. The nonzero (time-reversal even) component of the transverse polarization falls to zero as $p_T\sim O(m_\tau/E')$. Given the mass of $\tau$, the $\overset{(-)}{\nu}_\tau$ flux spectrum of Fig. 1, and the fact that the cross section rises very sharply from threshold ($E_{\text{th}}=3.5$ GeV) and assumes a linear growth with $E$ for $E\gtrsim 20$ GeV, most of the events are characterized by $m_\tau/E'\ll 1$ and hence $P_L(\tau^\pm)\simeq\pm1$.

In Fig. 3 we present several experimentally measurable distributions generated by our Monte Carlo calculation for the process (1.4). In order to facilitate comparison with experiment, our computations incorporate the typical experimental cuts $E_\mu>4$ GeV and $E_H>5$ GeV. Figure 3(a) shows the distributions in the muon, hadron, and visible energies, $E_\mu$, $E_H$, and $E_{\text{vis}}$, where $E_{\text{vis}}\equiv E_\mu+E_H$. In this graph and all the others where they appear, the solid and dashed curves apply for incident $\nu_\tau$ and $\bar\nu_\tau$, respectively. In graphs where only a solid curve is shown, the reason is that the differences between $\nu_\tau$ and $\bar\nu_\tau$ distributions are very small, indeed smaller than the estimated statistical uncertainty in the Monte Carlo calculation. The differences between the $\nu_\tau$ and $\bar\nu_\tau$ curves in Fig. 3 are easily understood. Because of the helicity effect, the $\tau^+$ carries off more energy than the $\tau^-$; to the extent that $m_\tau{}^2/(2m_NE)\ll 1$, one knows from neutrino scattering data that $\langle y\rangle_{\nu N}\sim 0.49$ and $\langle y\rangle_{\bar\nu N}\sim 0.33$. The finite mass of the $\tau$ reduces $\langle y\rangle$ for both $\nu_\tau$ and $\bar\nu_\tau$. Thus, $\langle y\rangle$ and hence, given that

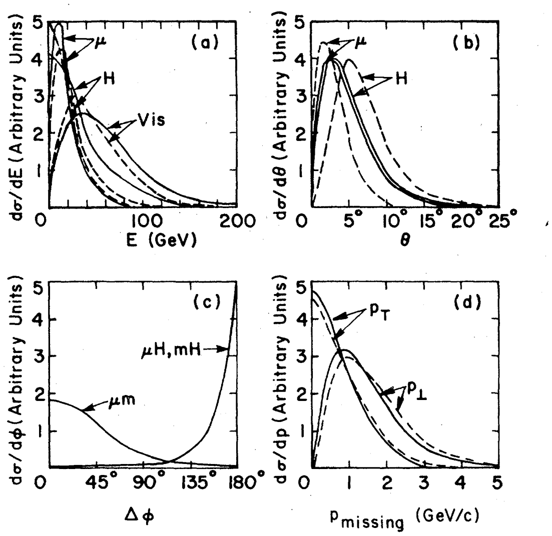


FIG. 3. Distributions in (a) the energies $E_\mu$, $E_H$, and $E_{vis}$; (b) the polar angles $\theta_\mu$ and $\theta_H$; (c) the azimuthal angles $\Delta\phi_{\mu H}$, $\Delta\phi_{mH}$, and $\Delta\phi_{\mu m}$; and (d) $(p_\perp)_{missing}$ and $(p_T)_{missing}$ for the processes [Eq. (1.4)] $\nu_\tau N \to \tau^- X$; $\tau^- \to \nu_\tau \mu^- \bar{\nu}_\mu$ (solid curves) and $\bar{\nu}_\tau N \to \tau^+ X$; $\tau^+ \to \bar{\nu}_\tau \mu^+ \nu_\mu$ (dashed curves). See text for definitions of these kinematic quantities. The plots incorporate the cuts $E_\mu > 4$ GeV and $E_H > 5$ GeV.

the $\nu_\tau$ and $\bar{\nu}_\tau$ fluxes are essentially the same, also $\langle E_H \rangle$, is expected to be somewhat larger for $\nu_\tau$ than for $\bar{\nu}_\tau$. This is verified by the actual Monte Carlo results. Next, in order to analyze the $E_\mu$ and $E_{vis}$ spectra, consider the decay of the $\tau$. Neglecting terms of order $(m_\mu/m_\tau)^2$, the differential decay spectrum in the $\tau$ rest frame, has the form

$$\frac{1}{\Gamma}\frac{\partial^2\Gamma}{\partial \cos\omega \partial z} \simeq z^2[(3-2z)+\xi|P_L|\cos\omega(1-2z)], \tag{3.14}$$

where

$$z \equiv \frac{E_\mu^*}{(E_\mu^*)_{max}}, \tag{3.15}$$

$$\cos\omega \equiv \vec{s}_\tau^{\,*}\cdot\hat{p}_\mu^*, \tag{3.16}$$

starred quantities refer to the $\tau$ rest frame, and $\xi = \pm 1$ for $\tau^\mp$. Since $\vec{s}^{\,*}(\tau^\pm) \simeq \pm\hat{p}_\tau$, the decay distribution has the form, for both $\tau^-$ and $\tau^+$,

$$\frac{\partial^2\Gamma}{\partial \cos\omega \partial z} \simeq z^2[(3-2z) - \hat{p}_\mu^*\cdot\hat{p}_\tau(1-2z)]. \tag{3.17}$$

Hence, in both cases, the $\mu^\pm$, especially if it has large $z$, is emitted preferentially along the direction $\hat{p}_\tau$ (and then is swept toward $\hat{n}_b$ by the Lorentz transformation to the laboratory frame). The differences in the $E_{\mu^\pm}$ spectra are thus determined mainly by the helicity effect of the primary $\overset{(-)}{\nu}_\tau \to \tau^\pm$ scattering process, so that $\langle E_{\mu^+}\rangle$ is slightly larger than $\langle E_{\mu^-}\rangle$, while $\langle E_{vis}(\nu_\tau)\rangle \gtrsim \langle E_{vis}(\bar{\nu}_\tau)\rangle$.

Figure 3(b) shows the distributions in the polar angles

$$\theta_\mu \equiv \cos^{-1}(\hat{p}_\mu\cdot\hat{n}_b) \tag{3.18}$$

and

$$\theta_H \equiv \cos^{-1}(\hat{p}_H\cdot\hat{n}_b) \tag{3.19}$$

for the signal process (1.4). The fact that $\theta(\mu^-) > \theta(\mu^+)$ is a consequence of the different $y$ dependence of $\tau^-$ versus $\tau^+$ production, as can be seen from the approximate expression, valid if $\delta_\tau \ll 1$, $\sin^2\theta_\tau/2 \simeq 0.5 m_N E^{-1} xy(1-y)^{-1}$. [The demonstration of the above ordering of polar angles also relies upon Eq. (3.17) as an intermediate step.] A similar argument shows that $\theta_H(\bar{\nu}_\tau) > \theta_H(\nu_\tau)$. So far, these distributions do not contain any striking features which could be used on an event-by-event basis to isolate the $\overset{(-)}{\nu}_\tau$ signal.

We next present in Fig. 3(d) the $(p_\perp)_{missing}$ and $(p_T)_{missing}$ distributions, given before,[4] which provided the foundation for the muon trigger test. The $(p_\perp)_{missing}$ curve peaks at ~0.75 GeV/$c$ but extends all the way out to ~5 GeV/$c$, while the $(p_T)_{missing}$ curve peaks at zero and extends out to about 3 GeV/$c$. The experimental uncertainty of ~0.5 GeV/$c$ in $(p_\perp)_{missing}$ is thus small compared to typical values of this quantity for the signal reaction. The reason that $dN/d(p_\perp)_{missing}$ peaks away from zero, whereas $dN/d(p_T)_{missing}$ peaks at zero is that the kinematic configuration in the $\vec{p}_\perp = 0$ corresponds to a single direction in phase space, viz. $\vec{p}_m \equiv \vec{p}(\overset{(-)}{\nu}_\tau) + \vec{p}(\overset{(-)}{\nu}_\mu) = \hat{n}_b$, whereas the configuration in which $\vec{p}_T = 0$ corresponds to a dense set of directions, with $\vec{p}_m$ lying in the apparent production plane defined by $\hat{n}_b$ and $\hat{p}_\mu$. There is thus more phase space available for the latter configuration than the former. Our studies of possible backgrounds indicate that they do not yield such large values of $(p_T)_{missing}$ and especially $(p_\perp)_{missing}$. Therefore, the cut $(p_\perp)_{missing} > 1$ GeV/$c$ can be used effectively to isolate the $\overset{(-)}{\nu}_\tau$ events from possible backgrounds. A cut $(p_T)_{missing} > 1$ GeV/$c$ would also be helpful, but somewhat less powerful because of the differences in the distributions discussed above.

Figure 3(c) shows the azimuthal-angle distributions $dN/d(\Delta\phi_{\mu H})$, $dN/d(\Delta\phi_{mH})$, and, in addition, $dN/d(\Delta\phi_{\mu m})$, where

$$\begin{aligned}\Delta\phi_{\mu m} &\equiv \sin^{-1}|(\hat{p}_\mu)_\perp \times (\hat{p}_\perp)_{missing}| \\ &= \pi - (\Delta\phi_{\mu H} + \Delta\phi_{mH}).\end{aligned} \tag{3.20}$$

The distributions are computed before imposing the $(p_\perp)_{missing} > 1$-GeV/$c$ cut. As was stressed in Ref. 4, these provide the second key discriminator in the test for $\overset{(}{\bar{\nu}}\overset{)}{_\tau}$ [especially after the application of the $(p_\perp)_{\text{missing}}$ cut; see below]. The peaking of the $\Delta\phi_{\mu H}$ and $\Delta\phi_{mH}$ distributions toward 180° is a result of the kinematics of the signal process: the $\tau$ and hadrons recoil away from each other on opposite sides of the beam direction, i.e., $(\vec{p}_\tau)_\perp = -(\vec{p}_H)_\perp$. When the $\tau$ decays, since $|\vec{p}_\mu^{\,*}| \ll |\vec{p}_\tau|$, again $(\hat{p}_\mu)_\perp \simeq -(\hat{p}_H)_\perp$, i.e., $\Delta\phi_{\mu H} \lesssim 180°$. Since also $|\vec{p}_i^{\,*}| \ll |\vec{p}_\tau|$, $i = \overset{(}{\bar{\nu}}\overset{)}{_\tau}$ or $\overset{(}{\bar{\nu}}\overset{)}{_\mu}$, $(\hat{p}_m)_\perp \simeq -(\hat{p}_H)_\perp$ so that $\Delta\phi_{mH} \lesssim 180°$. It follows, of course, that $dN/d(\Delta\phi_{\mu m})$ is maximal at $\Delta\phi_{\mu m} = 0$. The peaking in these azimuthal-angle distributions provides the basis for two further cuts to select $\overset{(}{\bar{\nu}}\overset{)}{_\tau}$ events.

Before presenting the azimuthal-angle distributions with the $(p_\perp)_{\text{missing}}$ cut imposed, it is of interest to examine the correlations between $(p_\perp)_{\text{missing}}$, $(p_T)_{\text{missing}}$, $\Delta\phi_{\mu H}$, and $\Delta\phi_{mH}$. Figure 4 shows these correlations. The scatter plots refer to the case of an incident $\nu_\tau$; the corresponding ones for $\bar{\nu}_\tau$ are quite similar and hence are not included. A clear correlation is apparent in these graphs: the larger the missing $p_\perp$ or $p_T$, the more tightly constrained $\Delta\phi_{\mu H}$ and $\Delta\phi_{mH}$ are to lie near 180°. This is an obvious consequence of the necessity of transverse-momentum balance among the totality of final-state particles. It is a very useful correlation, since it means that the cut $(p_\perp)_{\text{missing}} > 1$ GeV/$c$ [or a similar cut in $(p_T)_{\text{missing}}$] which is necessary as the first step in selecting $\overset{(}{\bar{\nu}}\overset{)}{_\tau}$ events, also serves to strengthen the peaking in $\Delta\phi_{\mu H}$ and $\Delta\phi_{mH}$ toward 180° and thereby increase the effectiveness of the azimuthal-angle distributions as indicators of genuine $\overset{(}{\bar{\nu}}\overset{)}{_\tau}$ events. To illustrate this concisely,

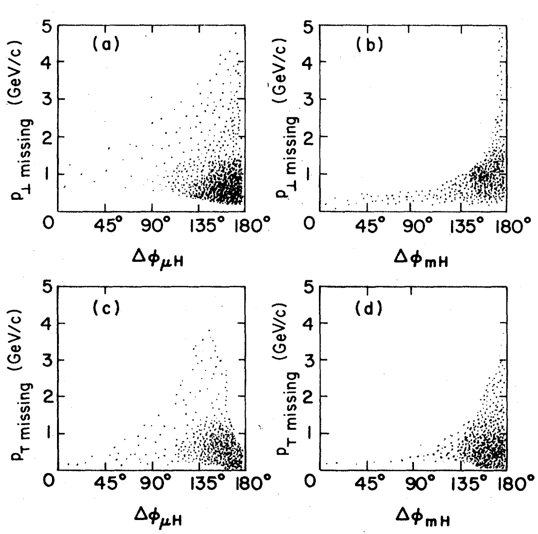


FIG. 4. Scatter plots showing correlations between $(p_i)_{\text{missing}}$, where $i=\perp$ or $T$, and $\Delta\phi_{jH}$, where $j=\mu$ or $m$, for process (1.4) with incident $\nu_\tau$. The plots incorporate the cuts $E_\mu > 4$ GeV and $E_H > 5$ GeV, as in Fig. 3.

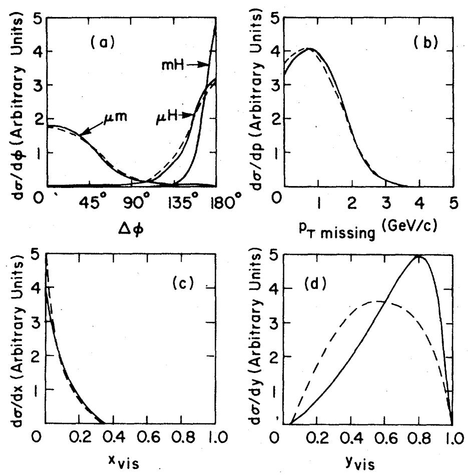


FIG. 5. Distributions in (a) the azimuthal angles $\Delta\phi_{\mu H}$, $\Delta\phi_{mH}$, and $\Delta\phi_{\mu m}$; (b) $(p_T)_{\text{missing}}$; (c) $x_{\text{vis}}$; and (d) $y_{\text{vis}}$ for the reaction and decay chain (1.4) with incident $\nu_\tau$ (solid curves) and $\bar{\nu}_\tau$ (dashed curves). The cuts applied are $E_\mu > 4$ GeV, $E_H > 5$ GeV, and, in addition, $(p_\perp)_{\text{missing}} > 1$ GeV/$c$.

Fig. 5(a) shows the azimuthal-angle distributions with the cut $(p_\perp)_{\text{missing}} > 1$ GeV/$c$ imposed. The $dN/d(\Delta\phi_{\mu H})$ curve decreases to small values for $\Delta\phi_{\mu H} \lesssim 90°$, while the $dN/d(\Delta\phi_{mH})$ curve is very sharply peaked, falling to zero for $\Delta\phi_{mH} \lesssim 120°$. These characteristics of the azimuthal-angle distributions provide the basis for the two cuts which constitute step (4) of the muon trigger test, namely $\Delta\phi_{\mu H} > 90°$ and $\Delta\phi_{mH} > 120°$ [after the events have passed the $(p_\perp)_{\text{missing}}$ cut in step (3)]. The distributions shown in Figs. 3(d) and 5(a) are the most important graphs presented in this paper, since their features serve as the foundation of the muon-trigger test.

Proceeding onward, in Fig. 5(b) we show the $dN/d(p_T)_{\text{missing}}$ distribution calculated with the $(p_\perp)_{\text{missing}} > 1$-GeV/$c$ cut imposed. As expected, this cut shifts the $(p_T)_{\text{missing}}$ curve to larger values than in Fig. 3(d). Figure 5(c) is a graph of the $x_{\text{vis}}$ distribution, where

$$x_{\text{vis}} \equiv \frac{Q_{\text{vis}}^{\,2}}{2m_N E_H} \tag{3.21}$$

and

$$Q_{\text{vis}}^{\,2} \equiv 4E_{\text{vis}}E_\mu \sin^2(\theta_\mu/2)\,. \tag{3.22}$$

This graph shows that for both $\nu_\tau$ and $\bar{\nu}_\tau$, $x_{\text{vis}}$ is confined to very small values. Next, Fig. 5(d) shows the $y_{\text{vis}}$ distributions for incident $\nu_\tau$ and $\bar{\nu}_\tau$, where

$$y_{\text{vis}} \equiv \frac{E_H}{E_{\text{vis}}}\,. \tag{3.23}$$

As has been pointed out before,[38] in a reaction where a heavy lepton such as $\tau^\pm$ is produced and decays (via the muon channel), $y_{\rm vis}$ is larger than the corresponding $y$ values for regular $\nu_\mu$ or $\bar\nu_\mu$ reactions, respectively. This is a result of the fact that a substantial fraction of the actual energy is carried off by the two unobserved neutrinos, so that $E_{\rm vis}$ is considerably smaller than the true $E$. This effect completely dominates over the countervailing tendency of $E_H$ to be somewhat smaller, for a given $E$, than in regular $\nu_\mu$ or $\bar\nu_\mu$ reactions, respectively. One can see from Fig. 5(d) that $dN/dy_{\rm vis}$ peaks at $y_{\rm vis}$ ~0.8 for $\nu_\tau$ and $y_{\rm vis}$ ~ 0.6 for $\bar\nu_\tau$. This difference is a consequence of the properties that, for the same initial energy $E$, (a) $E(\tau^+) > E(\tau^-)$, so that $E(\bar\nu_\tau)_{\rm missing} > E(\nu_\tau)_{\rm missing}$, and (b) $E_H(\nu_\tau) > E_H(\bar\nu_\tau)$. Both the $\nu_\tau$ and $\bar\nu_\tau$ curves are distinctly different from $y$ distributions for the corresponding charged current $\overset{(-)}{\nu}_\mu$ reactions, most notably as $y_{\rm vis} \to 0$. Hence, given the primary $(p_\perp)_{\rm missing}$ and $\Delta\phi_{\mu H,\, mH}$ cuts, the $y_{\rm vis}$ distribution can serve as a useful means of confirming that the sample of events is due to incident $\overset{(-)}{\nu}_\tau$. Indeed, one could optionally impose a weak cut $y_{\rm vis} > 0.25$ on the $\overset{(-)}{\nu}_\tau$ sample.

We next present several interesting correlations among the various kinematic quantities, calculated with the $(p_\perp)_{\rm missing} > 1$-GeV/$c$ cut incorporated. Figure 6 shows that the larger $E_\mu$ or $E_H$ is, the smaller the angles $\theta_\mu$ and $\theta_H$ tend to be. From Fig. 7 one sees that as $E_\mu$ or $E_H$ is increased, $\Delta\phi_{\mu H}$ and $\Delta\phi_{mH}$ are pushed closer to 180°. Finally, the correlations among the angles which are evident in Fig. 8 indicate that larger values of $\theta_\mu$ or $\theta_H$ are accompanied by values of $\Delta\phi_{\mu H}$ and $\Delta\phi_{mH}$ which are closer to 180°. Furthermore, these

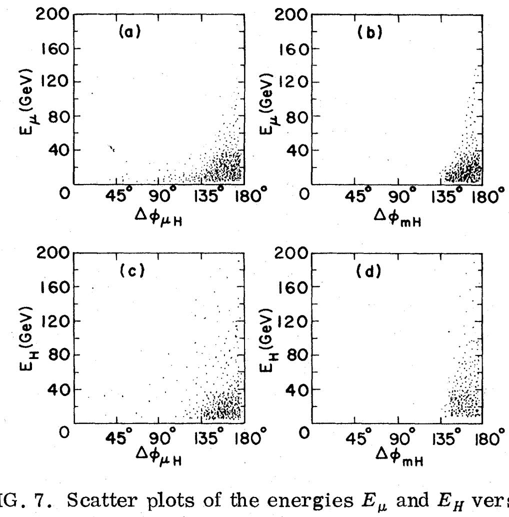

FIG. 7. Scatter plots of the energies $E_\mu$ and $E_H$ versus the azimuthal angles $\Delta\phi_{\mu H}$ and $\Delta\phi_{mH}$ for the process (1.4) with incident $\nu_\tau$. The cuts applied are the same as in Fig. 5.

scatter plots show the more severe falloff in the $\Delta\phi_{mH}$ distribution away from 180°, as compared with the falloff in the $\Delta\phi_{\mu H}$ distribution. These graphs, then, complete our Monte Carlo-generated plots of experimentally accessible quantities for the signal reaction and decay chain (1.4).

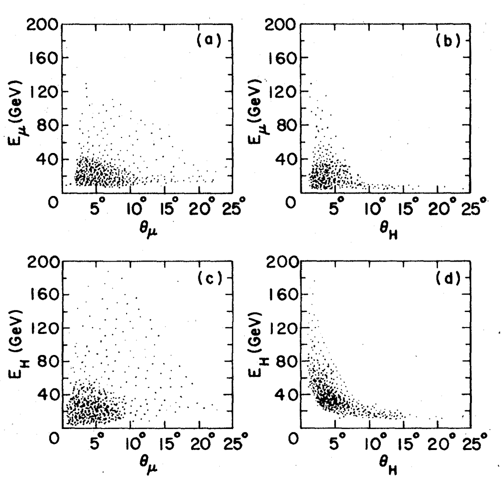

FIG. 6. Scatter plots of the energies $E_\mu$ and $E_H$ versus the polar angles $\theta_\mu$ and $\theta_H$ for process (1.4) with incident $\nu_\tau$. The cuts applied are the same as in Fig. 5.

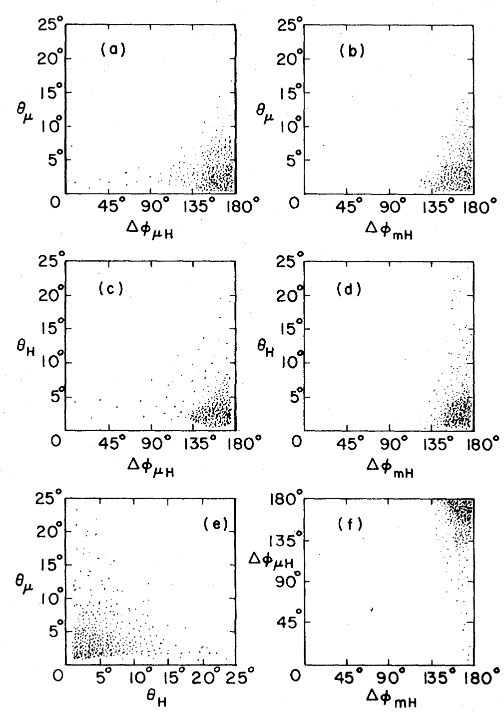

FIG. 8. Scatter plots showing the correlations between the various polar and azimuthal angles for process (1.4) with incident $\nu_\tau$. The cuts are the same as in Fig. 5.

In order to conclude that an observed sample of events which satisfy the trigger and cuts on $E_\mu$, $E_H$ (optionally, $\theta_\mu$), $(p_\perp)_{\text{missing}}$, $\Delta\phi_{\mu H}$, and $\Delta\phi_{mH}$ is due to incident $\overset{(-)}{\nu}_\tau$, it is necessary to show that no background processes could have produced a significant fraction of these events. This demonstration was carried out in Ref. 4. Here we shall review it and add some new, more detailed results on the background due to single charm production. The main physics backgrounds arise from the $\overset{(-)}{\nu}_e$ and $\overset{(-)}{\nu}_\mu$ coming from the beam dump. The first of these is comprised of neutral-current reactions in which very slow $\pi$'s and $K$'s in the leptonic spray decay leptonically (or, for $K$'s, semileptonically). This is a negligible background, since in order to decay in the volume of the detector the $\pi$'s and $K$'s would have to have energies so low that the resultant muon energies would fail the cut $E_\mu > 5$ GeV. Since the $\mu^\pm$ follows the direction $\hat{p}_H$, $\Delta\phi_{\mu H}$ would be small and would fail the special cut $\Delta\phi_{\mu H} > 90°$. Other standard techniques for eliminating this background are the measurement of the longitudinal uniformity of candidate events in the detector and variation of the density of the target material.

A second possible source of background arises from neutral-current $\overset{(-)}{\nu}_e$ or $\overset{(-)}{\nu}_\mu$ reactions, accompanied by associated charm production, in which one of the charmed hadrons decays (semi)-leptonically, yielding $\mu^\pm \overset{(-)}{\nu}_\mu$ + possible hadrons. Again, this process is negligible because, as has been shown experimentally and theoretically, the rate of associated charm production and single semileptonic decay is of order $\lesssim 10^{-4}$ relative to the corresponding neutral (or charged) current process.[39] We estimate that even before one imposes the special cuts which are part of the muon trigger test, the rate for this background, relative to the signal, is $\lesssim 10^{-2}$. Furthermore, the characteristics of these events are distinctively different from those of the signal. Most notably, $\Delta\phi_{\mu H}$ is peaked toward 0°, as was the case with the first type of background, so that this already small source of background can be further severely reduced by the cut $\Delta\phi_{\mu H} > 90°$.

The third and largest (although still unimportant) physics background, consists of the elementary charged-current reactions

$$\nu_{l_1} + (s \text{ or } d) \to l_1^- + c \searrow s + l_2^+ + \nu_{l_2} \tag{3.24}$$

and

$$\bar{\nu}_{l_1} + \bar{s} \to l_1^+ + \bar{c} \searrow \bar{s} + l_2^- + \bar{\nu}_{l_2}\,, \tag{3.25}$$

where

$$l_1, l_2 = \begin{cases} \text{(a) } e, \mu \\ \text{(b) } \mu, e\,. \end{cases} \tag{3.26}$$

These reactions will sometimes satisfy the trigger and usual cuts on $E_\mu$, $E_H$ (and optionally, $\theta_\mu$) if the muon energy is sufficiently high and the electron shower cannot be distinguished as such, in which case the experiments would not be able to tell if the electron were present. The probability $\delta_e$ that the electron shower will be misidentified as hadronic is greatest for case (b) where the electron is slow and is emitted as part of the hadron shower rather than directly from the leptonic vertex, as in case (a). It is expected[7] that in the CHARM, FMMN, and MOW experiments which may be capable of performing our test, $\delta_e \sim 0.1$ for case (a) and $\delta_e \sim 1$ for case (b). In Ref. 4 it was roughly estimated that *before* special cuts on $(p_\perp)_{\text{missing}}$, $\Delta\phi_{\mu H}$, and $\Delta\phi_{mH}$, assuming $N(\overset{(-)}{\nu}_\tau)/N(\overset{(-)}{\nu}_{\mu,e}) \sim 0.06$, the reactions of types (a) and (b) might contribute about 5% and 50% as many events, respectively, as the corresponding signal reactions with incident $\nu_\tau$ and $\bar{\nu}_\tau$. It was commented that the set of cuts which comprise the muon trigger test would further severely suppress this background. Here we can be more quantitative.

We consider the single charm production backgrounds to both the $\nu_\tau$- and $\bar{\nu}_\tau$- induced signal reactions, but for brevity only show distributions for the former case. This background arises from reaction (3.24) of type (b) and reaction (3.25) of type (a), both of which yield $\mu^- e^+$ final states. We have carried out a Monte Carlo simulation of these two reactions, folding in the $\nu_e$ and $\bar{\nu}_\mu$ fluxes computed by Mori (see Fig. 1). The resulting distributions in $(p_\perp)_{\text{missing}}$ and the azimuthal angles are presented in Figs. 9(a), 9(b) for reaction (3.24) of type (b) and in Figs. 9(c), 9(d) for reaction (3.25) of type (a). The azimuthal-angle plots are calculated with the $(p_\perp)_{\text{missing}} > 1\text{-GeV}/c$ cut applied. In the case of reaction (3.25) [or (3.24)] of type (a), in ~90% of the events the electron will be detected and the event will immediately be vetoed in the first step of the test. We are therefore concerned only with the small fraction in which the electron is not detected. Typically this will be a result of the electron being emitted at a relatively small scattering angle or having rather low energy. Thus a plausible functional form for the misidentification probability $\delta_e$ is $\delta_e \sim 0.1\theta(\theta_e^0 - \theta_e)\theta(E_e^0 - E_e)$, where $\theta(x) \equiv 1$ or 0 if $x > 0$ or $x < 0$, respectively, and $\theta_e^0$ and $E_e^0$ are roughly the values of $\theta_e$ and $E_e$ at which the probability function $\delta_e$ assumes half its maximum value, 0.1. In order to simulate the worst possible case, we have instead simply taken $\delta_e = 0.1$, independent of $\theta_e$ and $E_e$. It was expected[4,40] that the missing transverse momentum

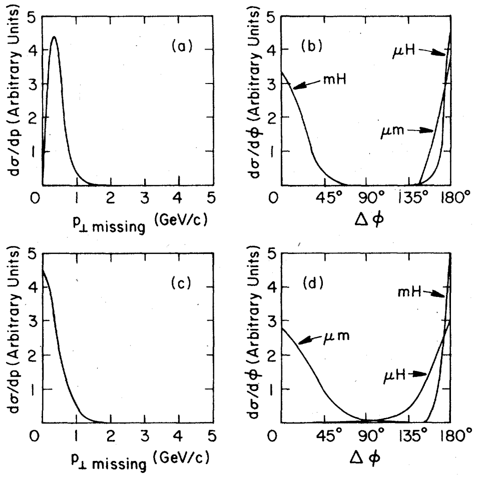


FIG. 9. Distributions in (a) $(p_\perp)_{\rm missing}$; and (b) $\Delta\phi_{\mu H}$, $\Delta\phi_{mH}$, and $\Delta\phi_{\mu m}$ for the background process [Eq. (3.24), type (b)] $\nu_\mu(d,s)\to\mu^- c$; $c\to(s,d)e^+\nu_e$. The azimuthal-angle distributions incorporate the cut $(p_\perp)_{\rm missing}>1$ GeV/$c$. Analogous distributions are presented in graphs (c) and (d) for the background process [Eq. (3.25), type (a)] $\bar\nu_e\bar s\to e^+\bar c$; $\bar c\to(\bar s,\bar d)\mu^-\bar\nu_\mu$. In all cases $\delta_e=1$, i.e., the electron is misidentified as part of the hadron shower.

would be substantially smaller for this general kind of background than for the signal process, because (1) there is only one unobserved neutrino rather than two as in the case of $\tau$ decay, and (2) since the transverse momentum of the total hadronic shower must balance that of the outgoing lepton, and since the charmed hadron comprises only one member of this hadronic shower, it carries less $p_\perp$ (for the same incident $E$) than the $\tau$ does in the signal process. As can be seen by comparing Fig. 3(d) with Figs. 9(a) and 9(c), our results confirm this expectation. We stress that the true values of $(p_\perp)_{\rm missing}$ for reaction (3.25) of type (a) are even smaller than those shown in Fig. 9(c) because of the $\theta_e$ dependence of $\delta_e$. Only 6.7% of the events in Fig. 9(a) and 1.4% of those in Fig. 9(c) survive the $(p_\perp)_{\rm missing}>1$-GeV/$c$ cut. For reference, the corresponding numbers for reaction (3.24) of type (a) and reaction (3.25) of type (b) are 4.0% and 2.6%, respectively.

As regards the azimuthal-angle distributions, in reaction (3.24) [or (3.25)] of type (b), since the neutrino follows the direction of the hadron spray, $\hat p_H$, $\Delta\phi_{mH}\sim 0°$ rather than 180°, in sharp contrast with the signal process (2c). Furthermore, the $\mu$ is emitted on the opposite side of the beam direction from the hadron shower, i.e., $(\vec p_\mu)_\perp=-(\vec p_H)_\perp$, so that, although $\Delta\phi_{\mu H}$ is peaked toward 180°, which is similar to the $\overset{(-)}{\nu}_\tau$ signal, the angle $\Delta\phi_{\mu m}$ tends to be near 180° rather than 0°, which is opposite to its behavior for the signal. These features are evident in Fig. 9(b). Thus this type of background can be further strongly suppressed by the cuts $\Delta\phi_{mH}>120°$ and $\Delta\phi_{\mu m}<90°$ (although not by the cut $\Delta\phi_{\mu H}>90°$). In the case of reaction (3.25) [or (3.24)] of type (a), for the only events which will constitute a background, i.e., those in which the electron shower is misidentified as part of the hadron shower, the apparent total hadronic momentum, $(\vec p_H)_{\rm vis}$, will differ substantially from the true $\vec p_H$. Indeed, the apparent azimuthal-angle distribution, shown in Fig. 9(d), will look somewhat like that for the signal process. It should again be remarked, however, that Fig. 9(d) represents the most pessimistic case; in fact, since electron misidentification selects small $\theta_e$ and $E_e$, the actual $\Delta\phi_{\mu H}$ and $\Delta\phi_{mH}$ curves for this type of background are not as sharply peaked toward 180° as those shown in this figure. In contrast, the $\Delta\phi_{\mu m}$ curve does not depend strongly on the fuctional form of $\delta_e$ and is accordingly an accurate indication of the behavior of this angle, which is small because the $\mu^+$ and $\nu_\mu$ are both emitted in the hadronic shower and follow its direction.

We have computed the total contribution of the third type of background using the Mori fluxes of Fig. 1 (see Ref. 35) and the measured dilepton rate due to charm production of ~0.5% for both $\nu_\mu$ and $\bar\nu_\mu$. Normalizing to 10 000 $\nu_\mu N\to\mu^- X$ events, we find that with the $(p_\perp)_{\rm missing}>1$-GeV/$c$ cut but *without* any azimuthal-angle cuts or any cuts on $E_\mu$ or $E_H$, there are (1) 3.4 events due to reaction (3.24) of type (b); (2) 0.02 events due to reaction (3.25) of type (a); (3) 0.1 events due to reaction (3.24) of type (a); and (4) 0.4 events due to reaction (3.25) of type (b). In contrast, as is shown in Table I, before the $(p_\perp)_{\rm missing}$ cut there are 40 $\nu_\tau N\to\tau^- X$; $\tau^-\to\nu_\tau\mu^-\bar\nu_\mu$ events and 15 $\bar\nu_\tau N\to\tau^+X$; $\tau^+\to\bar\nu_\tau\mu^+\nu_\mu$ events. The cut $(p_\perp)_{\rm missing}>1$ GeV/$c$ reduces these numbers to ~20 and ~7, respectively. It is evident from a comparison of Fig. 3(c) with Figs. 9(b) and 9(d), that the application of the azimuthal-angle cuts $\Delta\phi_{\mu H}>90°$, $\Delta\phi_{mH}>120°$, and $\Delta\phi_{\mu m}<90°$ will further reduce the background, by perhaps a factor of 10. It is expected therefore that after these cuts, the ratio of this third type of background to the $\overset{(-)}{\nu}_\tau$ signal should be of order a few percent.

Any exclusive charm production channels will contribute only a small fraction of the inclusive cross section which has just been discussed above. For example we estimate the rate, relative to the signal, for the diffractive process $\overset{(-)}{\nu}_l N\to l^\pm F^* X$ (where $l=e$ or $\mu$); $F^*\to F\gamma$; $F^\pm\to\tau^\pm\overset{(-)}{\nu}_\tau$; $\tau^\pm\to\overset{(-)}{\nu}_\tau X$ to be $\lesssim 1\%$. This small rate can be further strongly suppressed by the cut $\Delta\phi_{mH}>120°$ and, optionally a cut on $Q_{\rm vis}^2$.

There may well be more than three doublets of

TABLE I. Relative event rates in a beam-dump experiment, normalized to 10 000 $\nu_\mu N \to \mu^- X$ events, as computed without imposing any cuts and with the Mori (anti)neutrino fluxes of Ref. 35. These are applicable for 400-GeV protons incident on a copper beam dump, followed by a detector 250 m downstream which subtends an angle of 0 to 2 mrad.

| Reaction | Number of events |
|---|---|
| $\nu_\mu N \to \mu^- X$ | 10 000 |
| $\bar\nu_\mu N \to \mu^+ X$ | 3 400 |
| $\nu_e N \to e^- X$ | 7 200 |
| $\bar\nu_e N \to e^+ X$ | 3 000 |
| $\nu_\tau N \to \tau^- X, \tau^- \to \nu_\tau$ + hadrons | 120 |
| $\nu_\tau N \to \tau^- X, \tau^- \to \nu_\tau e^- \bar\nu$ | 40 |
| $\nu_\tau N \to \tau^- X, \tau^- \to \nu_\tau \mu^- \bar\nu_\mu$ | 40 |
| $\bar\nu_\tau N \to \tau^+ X, \tau^+ \to \bar\nu_\tau$ + hadrons | 45 |
| $\bar\nu_\tau N \to \tau^+ X, \tau^+ \to \bar\nu_\tau e^+ \nu_e$ | 15 |
| $\bar\nu_\tau N \to \tau^+ X, \tau^+ \to \bar\nu_\tau \mu^+ \nu_\mu$ | 15 |
| $\sum_i (\nu_i N \to \nu_i X),\ i = e, \mu, \tau$ | 5 100 |
| $\sum_i (\bar\nu_i N \to \bar\nu_i X),\ i = e, \mu, \tau$ | 2 300 |

leptons (and correspondingly, of quarks) in the standard model.[41] One might, therefore, worry that an apparent signal due to process (1.4) could contain a significant admixture of events from the analogous processes $\overset{(-)}{\nu}_i N \to l_i^\pm X$; $l_i^\pm \to \overset{(-)}{\nu}_i \mu^\pm \overset{(-)}{\nu}_\mu$, where $i = 4, \ldots, n$, with $n$ denoting the number of doublets. However, recapitulating the discussion in Ref. 4, it is easy to show that this is not the case. In order for there to be a non-negligible flux of $\overset{(-)}{\nu}_i$, $i = 4, \ldots, n$, these (anti)neutrinos must be produced via leptonic decays of $F$ or $D$ mesons. But, given the present lower limits on the mass of $l_4$ (where the $l_i$ are arranged in order of increasing mass), this is impossible. Specifically, these limits are[13] $m(l_4) \gtrsim 3.5$ GeV from the measurement of

$$R \equiv \sigma(e^+e^- \to \text{hadrons})/\sigma(e^+e^- \to \mu^+\mu^-)$$

up to $\sqrt{s} \simeq 7$ GeV, and, tentatively, $m(l_4) \gtrsim 8$ GeV from the preliminary measurements of $R$ at $\sqrt{s} = 13$ and 17 GeV at PETRA.[42] Hence, the additional neutrinos $\nu_i$, $i = 4, \ldots, n$, would have to be produced via (1) the Drell-Yan process $pN \to l_i^+ l_i^- X$; $l_i^\pm \to \overset{(-)}{\nu}_i X'$; (2) the weak analog of the Drell-Yan reaction, $pN \to Z_{\text{virtual}}$ + anything; $Z_{\text{virtual}} \to \nu_i \bar\nu_i$, which avoids the kinematic suppression incurred by the necessity of producing an $l_i^+ l_i^-$ pair in mechanism (1), but suffers a reduction in rate by $\sim G_F^2 s/\alpha^2$; or (3) (semi)leptonic decays of hadrons which, judging from the preliminary PETRA results, must contain a quark considerably heavier than the $\Upsilon$-constituent quark $b$. Thus, simply for kinematic reasons, the flux of any such additional (anti)neutrinos $\overset{(-)}{\nu}_i$, $i = 4, \ldots, n$, would be negligible compared to that of $\overset{(-)}{\nu}_\tau$. This comment also applies to the two other tests for $\overset{(-)}{\nu}_\tau$ to be discussed in Sec. IV, the double shower and $R_{\text{NC/CC}}$ tests; if they were feasible at all, they would be specific to $\overset{(-)}{\nu}_\tau$.

In addition to these conventional physics backgrounds, there is also a background arising from the imperfect accuracy with which the experiments can measure $\vec{p}_H$ and thereby test for missing transverse momentum. (The measurement errors in $\vec{p}_\mu$ are small compared to those in $\vec{p}_H$.) To assess the characteristics and importance of this source of background is necessarily a task for the specific experimental groups which seek to perform our test. It cannot be too serious, given the estimate[7] of $\sim \pm 0.5$ GeV/$c$ as the net uncertainty in $(p_\perp)_{\text{missing}}$, the substantially larger values of $(p_\perp)_{\text{missing}}$ manifested by the $\overset{(-)}{\nu}_\tau$ signal events, as is evident from Fig. 3(d), and the proposed cut $(p_\perp)_{\text{missing}} > 1$ GeV/$c$. Although a detailed analysis of this background would require considering each particular experimental apparatus, one can make a generally applicable comment, namely that events with apparent missing $p_\perp$ due to measurement errors in $\vec{p}_\mu$ and/or $\vec{p}_H$ will not show the striking azimuthal-angle dependence of the signal events. Thus, while it is still true that $\Delta\phi_{\mu H}$ will be peaked toward 180°, there will not be any peaking of $\Delta\phi_{mH}$ toward 180°, or of $\Delta\phi_{\mu m}$ toward 0°.

Besides considering backgrounds due to conventional physical processes and to imperfect measurement accuracy, it is also necessary to demonstrate that an apparent $\overset{(-)}{\nu}_\tau$ signal could not arise from possible exotic processes. We have examined in turn (1) hypothetical charged and neutral heavy-lepton production; (2) the effects of a possible admixture of effectively stable neutral heavy leptons in the flux from the beam dump; and (3) the possibility that $\nu_\tau$ is not a sequential neutrino. As was discussed in Sec. I, there is strong indirect evidence against all of these processes and hypotheses.

Concerning (1), models[43] with ortho- and para-leptons are implausible because the masses of such particles are constrained to be rather large. Recent neutrino experimental results give $m(M^+_{\text{para}}) > 12$ GeV,[44] $m(M^-_{\text{ortho}}) > 9$ GeV[45,46] (similar limits have been placed by bubble-chamber data[47]). Moreover, $e^+e^-$ annihilation experiments[42] yield $m(E^\pm) \gtrsim 3.5$ GeV, and tentatively $\gtrsim 7$ GeV, which is consistent with the null effect[48] noticed in comparing the reactions $\overset{(-)}{\nu}_e Ne \to e^\pm X$ and $\overset{(-)}{\nu}_\mu Ne \to \mu^\pm X$. This same neutrino experiment provided good evidence against a light mass $E^0$. For $M^0$ leptons there is a mass limit[49-52] of $m(M^0) > 6$ GeV. Therefore, there will be strong kinematic suppression of heavy-lepton production[53] by neutrinos and this first type of background does not present any problem for the muon-trigger test.

Concerning (2), reactions which could be induced by an effectively stable neutral heavy lepton $L_s^0$ (where "$s$" denotes "stable") have been classified and studied previously.[54] Astrophysical limits[55] on the mass of this particle indicate that $m(L_s^0) \gtrsim 2$ GeV, so the $L_s^0$ could not be produced via the decays of $F$ and $D$ mesons, and the flux $N(\overset{(-)}{L}{}_s^0)$ from the beam dump would be negligible relative to $N(\overset{(-)}{\nu}_\tau)$. Independent of this, with an appropriately instrumented detector it would be possible to apply a timing test proposed previously[54] to identify and eliminate this background to the $\overset{(-)}{\nu}_\tau$ signal. The test relies upon measuring the local time delay between the arrival of the $L_s^0$'s at the detector, as determined by the direct muons which they produce, and a timing signal synchronized with the rf structure of the proton pulses from the accelerator. In passing, it may be noted that, in principle, this timing test can be applied to the signal events themselves to show that the "mass" of $\nu_\tau$[14] is consistent with being equal to zero.

As regards the third exotic type of background, when sufficiently accurate predictions of the $\overset{(-)}{\nu}_\tau$ flux become available, one will be able to use the muon trigger test to determine experimentally whether $\nu_\tau$ is a sequential neutrino. The indicator which will decide this question is simply the rate of signal $\overset{(-)}{\nu}_\tau$ events, relative to regular charged current $\overset{(-)}{\nu}_\mu$ events. Actually, as was discussed in Sec. I, the possibilities that $\nu_\tau = \bar{\nu}_l$, where $l=e$ or $\mu$, and that $\nu_\tau = \nu_\mu$, have already been ruled out by data on $\tau$ decay from $e^+e^-$ machines[1-3] and from high-energy neutrino experiments,[15] respectively. Let us therefore concentrate on the one remaining case which, if strongly disfavored by indirect evidence, has not been directly ruled out, namely that $\nu_\tau = \nu_e$. If $\nu_\tau$ is a sequential neutrino, then the ratio of signal events from process (1.4) to regular $\nu_\mu N \to \mu^- X$ events will be

$$\frac{R(\nu_\tau N \to \tau^- X; \tau^- \to \nu_\tau \mu^- \bar{\nu}_\mu)}{R(\nu_\mu N \to \mu^- X)} = \frac{\int dE N(\nu_\tau; E)\sigma(\nu_\tau N \to \tau^- X) B(\tau \to \nu_\tau \mu \bar{\nu}_\mu)}{\int dE\, N(\nu_\mu; E)\sigma(\nu_\mu N \to \mu^- X)} . \quad (3.27)$$

As computed in Table I (without any cuts), this ratio is equal to 0.004; with the $(p_\perp)_{\text{missing}}$ cut imposed it would be 0.002. The first number can be understood if one approximates Eq. (3.27) by $\sim(0.03)\times(0.7)\times(0.19) = 0.004$, where the factors in parentheses represent, respectively, the appropriately weighted ratio of $\nu_\tau$ and $\nu_\mu$ fluxes, an average kinematic suppression factor for $\tau$ production, and the branching ratio for the decay $\tau^\pm \to \overset{(-)}{\nu}_\tau \mu^\pm \overset{(-)}{\nu}_\mu$. If, on the other hand, $\nu_\tau = \nu_e$, then the rate of signal events would be significantly larger, because $N(\overset{(-)}{\nu}_e) \gg N(\overset{(-)}{\nu}_\tau)$. A crucial input here is the lower bound on the $\tau\nu_\tau$ coupling which has been established by the DELCO experiment,[2] viz. $g_{\tau\nu_\tau}{}^2 > 0.12 g_{l\nu_l}{}^2$, where $l=e$ or $\mu$.[56] We have computed the signal event rate using the fluxes of Fig. 1 and the hypothesis that $\nu_\tau = \nu_e$; the result (again, without cuts), normalized to 10 000 regular $\nu_\mu N \to \mu^- X$ events, with $g_{\tau\nu_\tau}{}^2 = (g_{\tau\nu_\tau}{}^2)_{\min}$, is 110 events. Thus, there would be at least a threefold increase in the $\nu_\tau$ signal event rate, up to the level of 0.011 times the $\nu_\mu N \to \mu^- X$ rate. The above number could be inferred from Table I; it is equal to $\sim(0.12)\times(0.67)\times(0.19)\times(7200)$, where the origin of the first three factors is clear, and the fourth is the number of events for the regular $\nu_e N \to e^- X$ reaction. There would also be a corresponding increase in the $\bar{\nu}_\tau$ signal event rate. In order to use the data to decide between these two possible assignments for $\nu_\tau$, it is necessary to have accurate predictions for the (anti)neutrino fluxes in a beam-dump experiment, and in particular, the relative sizes of $N(\overset{(-)}{\nu}_e)$, $N(\overset{(-)}{\nu}_\mu)$, and $N(\overset{(-)}{\nu}_\tau)$. At the present time, one does not have sufficiently accurate knowledge of the relative magnitudes of these fluxes; the most important sources of uncertainty are in the ratio of the differential and total cross sections for hadronic production of $F\bar{F}$ versus $D\bar{D}$ pairs, and in the branching ratio $B(F^\pm \to \tau^\pm \overset{(-)}{\nu}_\tau)$. We anticipate, however, that these inputs will eventually be measured with reasonable accuracy. Then, having (anti)neutrino flux calculations of requisite precision, one will be able to use the muon trigger test to determine whether $\nu_\tau$ is a sequential neutrino.

We next consider an interesting and entirely possible generalization of the standard model, namely one in which the neutrinos have nonzero and unequal masses. Then, in contrast to the usual massless case, the neutrino gauge group eigenstates could not be defined to be simultaneous mass eigenstates. Let us denote the former states by $\nu_i$, $i = e, \mu, \tau, \ldots, n \equiv 1, 2, 3, \ldots, n$, and the latter by $L_j^0$, $j = 1, 2, \ldots, n$. Then the mixing of the mass eigenstates to form gauge group eigenstates is specified by $\nu_i = U_{ij} L_j^0$, $i,j = 1, \ldots, n$, where $U$ is the (unitary) lepton mixing matrix. The constraints on such lepton mixing from quark-lepton and $e$-$\mu$ universality, nonobservation of neutrino oscillations, and nonobservation of $\mu$- and $e$-number nonconserving processes have been analyzed before in the case $n=3$, which is of greatest interest here.[57] These constraints force the matrix $U$ to be almost diagonal. It is true that a $\nu_i$, $i = e$, $\mu$, or $\tau$, which is produced in the beam dump will not remain a $\nu_i$, but rather the $n$ different mass eigenstates $L_j^0$ in the original combination $\nu_i = U_{ij} L_j^0$ will propagate differently. Moreover, these differences in propagation themselves vary as a function of the momentum of the initial $\nu_i$. But a point of principle should be stressed here: The validity of a test for $\nu_\tau$ is in no way affected by the existence of lepton mixing, since it is always a test for the gauge group eigenstate. Alternatively, if one views the object of the test as being the observation of the mass eigenstate $L_3^0$, then it is true that in the presence of mixing, one is no longer directly observing this particle. But this is an academic point, because even if, in fact, the off-diagonal elements of $U$ were as large as the diagonal ones, and a substantial part of the $\nu_\tau$ signal arose from incident $L_i^0$, $i=1$ and 2 (and, by oscillations $4, 5, \ldots, n$) one could still justifiably claim to have observed, albeit now indirectly, $L_3^0$. This follows because if $L_3^0$ did not exist, there would be no such mixing as specified by a unitary $n \times n$ matrix.

Finally, there remains the question of whether the total number of $\overset{(-)}{\nu}_\tau$ events will be large enough to obtain a reasonable sample in a typical experiment. In order to answer this question we first compute the numbers of events for various reactions, using the fluxes of Fig. 1 and normalizing to 10 000 $\nu_\mu N \to \mu^- X$ events. For the sake of generality no cuts are applied. The effect of the standard $E_H$ and, in the CC reactions also in the $E_\mu$, cuts would be to reduce somewhat, roughly uniformly, the numbers of events in the various types of reactions. For proper identification, the $\overset{(-)}{\nu}_\tau$ events must, of course, have a $(p_\perp)_{\text{missing}} > 1$-GeV/$c$ cut imposed; this reduces the $\nu_\tau$ and $\bar{\nu}_\tau$ samples each by roughly a factor of 2. To compute the absolute event rates, we consider a typical experiment with a ~200-ton detector located 250 m downstream from a copper beam dump. In normal running conditions there would be a total of ~$10^{18}$ 400-GeV protons incident on the target; using this number together with the Mori fluxes,[35] we estimate that there would be a total of ~5–20 000 $\nu_\mu N \to \mu^- X$ events in the raw data sample, where the range of a factor of 2 is intended to represent theoretical uncertainties in the calculation and the differences in geometry and acceptance among various types of beam-dump experiments. Hence, in such an experiment one should be able to obtain 25–50 $\overset{(-)}{\nu}_\tau$ events. We recall again that the $\overset{(-)}{\nu}_\tau$ curves in Fig. 1 are partial fluxes, computed by including only 68% of all of the $\tau$ decay modes, and should be increased by approximately 50% to estimate the total $\overset{(-)}{\nu}_\tau$ flux. Moreover, they are based on the conservative estimate of Ref. 4 that $\sigma(pN \to F\bar{F}X)/\sigma(pN \to D\bar{D}X) = 0.1$; this could easily be low by a factor of 3. Hence we anticipate that the $\overset{(-)}{\nu}_\tau$ yield may be somewhat larger than the number quoted above. Thus, our conclusion is that if, as planned, the experiments can achieve as good a measurement accuracy as ±0.5 GeV/$c$ in $(p_\perp)_{\text{missing}}$, then they should be able to apply our muon trigger test successfully to observe $\nu_\tau$ and $\bar{\nu}_\tau$, and should, with typical running conditions, gather a total $\overset{(-)}{\nu}_\tau$ sample which is large enough to allow a comparison of experimental spectral distributions with those calculated here.

## IV. OTHER TESTS FOR $\nu_\tau$ INTERACTIONS IN BEAM-DUMP EXPERIMENTS

In addition to our muon-trigger test, there are two other tests which one might consider for the purpose of observing $\nu_\tau$ interactions in a beam-dump experiment, but as we shall now show, neither of them has much chance of success.

### A. The double-shower or semileptonic-trigger test

One would like to exploit the semileptonic decay of the $\tau$ as well as its leptonic decay as a means of detection. The former decay mode, if usable, would ostensibly appear to have a rate advantage of about a factor of 3, since $B(\tau \to \nu_\tau + \text{hadrons}) \simeq 0.62$, whereas $B(\tau \to \nu_\tau \mu \bar{\nu}_\mu) \simeq 0.19$. Accordingly, we have studied the production and decay chain (1.2), and in Fig. 10(a) we present the results of a Monte Carlo simulation of this process which folds in the $\overset{(-)}{\nu}_\tau$ flux spectrum of Fig. 1 together with a cut $E_{\text{vis}} \equiv E_h + E_H > 5$ GeV. Figure 10(a) shows the distributions in $E_h$ and $E_H$, where $E_h$ is the energy of the hadron shower from the decay of $\tau$, and $E_H$,

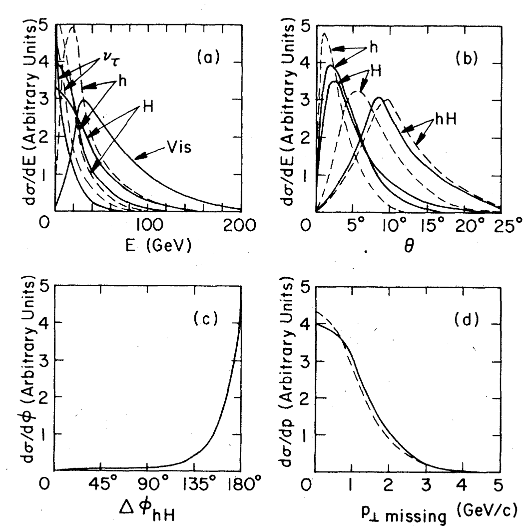


FIG. 10. Distributions in (a) the energies $E_{\nu_\tau}$, $E_h$, $E_H$, and $E_{\text{vis}}$; (b) the polar angles $\theta_h$, $\theta_H$, and $\theta_{hH}$; (c) the azimuthal angle $\Delta\phi_{hH}$; and (d) $(p_\perp)_{\text{missing}}$ for processes [Eq. (1.2)] $\nu_\tau N \to \tau^- X$; $\tau^- \to \nu_\tau X'$ (solid curves) and $\bar{\nu}_\tau N \to \tau^+ X$; $\tau^+ \to \bar{\nu}_\tau X'$ (dashed curves). The plots incorporate the cut $E_{\text{had}} \equiv E_h + E_H > 5$ GeV.

as defined before, is the energy of the shower from the primary hadron vertex. These are depicted separately for analytical purposes only; as will be seen below, it is not in general possible to separate these two showers. The total visible energy $E_{\rm vis}$ is also included in the graph. Because of the (single) outgoing neutrino from the semileptonic decay of the $\tau$, there is some missing transverse momentum, although it is not as large as in the muonic decay, where there are two outgoing neutrinos. This is clear from a comparison in Fig. 3(d) with Fig. 10(d), which shows the $dN/d(p_\perp)_{\rm missing}$ distribution for process (1.2). Since $\langle p_\perp\rangle_{\rm missing}$ is smaller in process (1.2) than in process (1.4), to be able to conclude experimentally that $(p_\perp)_{\rm missing} \neq 0$ requires a commensurately greater accuracy in the measurement of $p_H$. If one makes the same cut, $(p_\perp)_{\rm missing} > 1$ GeV/$c$ as in the muon-trigger test, a much larger fraction of genuine $\overset{(-)}{\nu}_\tau$ events will be rejected. Indeed, in sharp contrast to the muon-trigger test, the imposition of a $(p_\perp)_{\rm missing}$ cut here would severely *reduce*, rather than increase, the ratio of signal to background. The reason for this is the huge background of regular $\overset{(-)}{\nu}_e$ and $\overset{(-)}{\nu}_\mu$ neutral-current events, which in general have considerably larger $(p_\perp)_{\rm missing}$ than the signal events of process (1.2). Consequently, although there is missing transverse momentum in the signal events, it cannot be used as a primary selection criterion. The feature of process (1.2) which one must try to use, if possible, as a means of detection, is the characteristic that there are two hadron showers,[28] one from the primary hadronic vertex, and the other from the semileptonic decay of the $\tau$. If one were able to utilize this as a practical selection criterion, then a necessary last step to the test would be the requirement that there be substantial missing transverse momentum, $(p_\perp)_{\rm missing} > 1$ GeV/$c$. This would be essential in order to eliminate the large number of events due to the reaction $\overset{(-)}{\nu}_e N \to e^\pm X$ in which the electron shower is misidentified as a hadron shower. Although this is expected to occur in only about 10% of the $\overset{(-)}{\nu}_e N \to e^\pm X$ events, it would still be a very serious background since $N(\overset{(-)}{\nu}_e) \gg N(\overset{(-)}{\nu}_\tau)$.

The double-shower test then, consists of the requirements: (1) no outgoing $\mu$ with $E_\mu > 4$ GeV (the $E_\mu$ cut is applied to eliminate low-energy $\mu$'s from $\pi$ and $K$ decay); (2) the existence of two distinct hadron showers; and (3) if conditions (1) and (2) are satisfied, the final requirement that $(p_\perp)_{\rm missing} > 1$ GeV/$c$. The crucial question is whether the two showers in the production and decay chain (1.2) will be recognizably different on an event-by-event basis from the one shower in the far more plentiful regular $\overset{(-)}{\nu}_e$ and $\overset{(-)}{\nu}_\mu$ neutral-current reactions. One fundamental probelm is that the multiplicity of the hadron shower from $\tau$ decay is rather small; typically the number of the hadrons is ~1–3. Thus, it is not even clear that, given adequate angular resolution, it would be possible to identify these hadrons as the shower from the $\tau$. In order to study the angular separation of the two showers, we take the three-momentum of the $\tau$ shower to be the sum of the three-momenta of the quarks $q_1$ and $q_2$ in the decay $\tau \to \nu_\tau q_1 \bar{q}_2$ where $q_1 = d$ or $s$ and $q_2 = u$: $\vec{p}_h \equiv \vec{p}(q_1) + \vec{p}(q_2)$. Then the polar opening angle of the $\tau$ shower, with respect to the beam direction $\hat{n}_b$ is

$$\theta_h \equiv \cos^{-1}(\hat{p}_h \cdot \hat{n}_b)\,. \tag{4.1}$$

In Fig. 10(b) we plot the distributions in opening angles of the $\tau$ and primary hadron showers, $\theta_h$ and $\theta_H$, respectively. Because of the outgoing neutrino, the two showers do not emerge exactly on opposite sides of the beam direction. However, just as the final muon and neutrinos were swept in the direction of the recoiling $\tau$ so that $\Delta\phi_{\mu H} \lesssim 180°$ and $\Delta\phi_{mH} \lesssim 180°$ in process (1.4), so also here the neutrino and hadrons from the $\tau$ decay are swept in the direction of the initial $\tau$ recoil, and hence the distribution in the azimuthal angle $\Delta\phi_{hH}$ relative to the beam axis, between the $\tau$ shower and primary hadron shower, shown in Fig. 10(c), is sharply peaked toward 180°. That is, the two showers emerge almost, although not exactly, on opposite sides of the beam direction. Hence, the total opening angle $\theta_{hH} \lesssim \theta_h + \theta_H$. As is evident in Fig. 10(b), the distribution $dN/d\theta_{hH}$ peaks at ~8° and ~10° for incident $\nu_\tau$ and $\bar{\nu}_\tau$, respectively. Unfortunately, the typical angular spread of the hadron shower in neutrino reactions is ~20°–30°. Thus the angular separation of the two showers is generally small compared to their angular spread, and consequently the double-shower test fails as a means of detecting $\nu_\tau$ interactions. This failure emphasizes a key advantage of the muon-trigger test: Since the trigger is more restrictive and, in particular, since it requires an outgoing muon, the test is more powerful, yields more information, and is more free from backgrounds.

### B. The anomalous $R_{\rm NC/CC}$ test

An important feature of the $\nu_\tau$ and $\bar{\nu}_\tau$ neutral-current (NC) and charged-current (CC) reactions (1) and (2) is that the apparent ratio of NC to CC cross sections is much larger than the corresponding ratios for $\nu_\mu$ and $\bar{\nu}_\mu$ reactions. This is a consequence of the fact that if the $\tau^\pm$ decays semileptonically and also, in a conventional detector, if it decays to $\overset{(-)}{\nu}_\tau e^\pm \overset{(-)}{\nu}_e$, the event will appear to be an NC event. However, one cannot directly measure the ratios of NC to CC cross sections, or even event rates, for processes (1) and (2) in isolation. One might hope, that although the $\overset{(-)}{\nu}_\tau$ flux is relatively small, this effect would still serve as a practical means for establishing the presence of an admixture of $\overset{(-)}{\nu}_\tau$ in the neutrino flux from the beam dump. Even if it were feasible, this test could not be used on an event-by-event basis, and would yield less information compared to the two other tests.

We have studies the feasibility of the anomalous $R_{NC/CC}$ test, using the flux spectra of Fig. 1, and we find that even in the ideal case of a detector which can distinguish electrons from hadrons, the increase in the apparent NC to CC event rate due to $\overset{(-)}{\nu}_\tau$ is too small for the test to be usable. The apparent or effective CC and NC event rates are

$$R_{CC}(E)=N(\nu_\mu)\sigma_{CC}(\nu_\mu)+N(\bar\nu_\mu)\sigma_{CC}(\bar\nu_\mu)+[N(\nu_e)\sigma_{CC}(\nu_e)+N(\bar\nu_e)\sigma_{CC}(\bar\nu_e)](1-\delta_e)$$
$$+[N(\nu_\tau)\sigma_{CC}(\nu_\tau)+N(\bar\nu_\tau)\sigma_{CC}(\bar\nu_\tau)][B_\mu+B_e(1-\delta_e)] \tag{4.2}$$

and

$$R_{NC}(E)=N(\nu_\mu)\sigma_{NC}(\nu_\mu)+N(\bar\nu_\mu)\sigma_{NC}(\bar\nu_\mu)+N(\nu_e)[\sigma_{NC}(\nu_e)+\sigma_{CC}(\nu_e)\delta_e]+N(\bar\nu_e)[\sigma_{NC}(\bar\nu_e)+\sigma_{CC}(\bar\nu_e)\delta_e]$$
$$+[N(\nu_\tau)\sigma_{CC}(\nu_\tau)+N(\bar\nu_\tau)\sigma_{CC}(\bar\nu_\tau)][1-B_\mu-B_e(1-\delta_e)]+[N(\nu_\tau)\sigma_{NC}(\nu_\tau)+N(\bar\nu_\tau)\sigma_{NC}(\bar\nu_\tau)]\,, \tag{4.3}$$

where $\sigma_{CC}(\overset{(-)}{\nu}_l)\equiv\sigma(\overset{(-)}{\nu}_l N\to l^\pm X)$, $\sigma_{NC}(\overset{(-)}{\nu}_l)\equiv\sigma(\overset{(-)}{\nu}_l N\to\overset{(-)}{\nu}_l X)$, $B_l\equiv B(\tau\to\nu_\tau l\nu_l)$ (with[1-3] $B_e\simeq B_\mu\simeq 0.19$), and the energy dependence of the fluxes and cross sections is implicit in the notation. In Eqs. (4.2) and (4.3) we have further made the approximation of using the same $E$-independent electron misidentification probability $\delta_e$ for $\overset{(-)}{\nu}_e$- and $\overset{(-)}{\nu}_\tau$-induced reactions. This has no effect on our conclusions. Since in the NC and $\nu_\tau$ CC reactions one cannot reconstruct the incident energy and since, in any case, in this test one cannot measure any of the individual event rates on the right-hand sides of Eqs. (4.2) and (4.3), the most that can be obtained experimentally is the ratio of total apparent NC-to-CC event rates

$$R_{NC/CC}\equiv\frac{\int R_{NC}(E)dE}{\int R_{CC}(E)dE}\,. \tag{4.4}$$

We have calculated this ratio for the cases of zero and perfect electron detection capability ($\delta_e=1$ and 0, respectively). We find that if there were no $\overset{(-)}{\nu}_\tau$ flux,

$$R_{NC/CC}(N(\overset{(-)}{\nu}_\tau)=0;\delta_e=1)=1.74\,, \tag{4.5a}$$

$$R_{NC/CC}(N(\overset{(-)}{\nu}_\tau)=0;\delta_e=0)=0.72\,, \tag{4.5b}$$

whereas for the expected $\overset{(-)}{\nu}_\tau$ fluxes,

$$R_{NC/CC}(N(\overset{(-)}{\nu}_\tau)_{calc}\,;\delta_e=1)=1.75\,, \tag{4.6a}$$

$$R_{NC/CC}(N(\overset{(-)}{\nu}_\tau)_{calc}\,;\delta_e=0)=0.75\,. \tag{4.6b}$$

Thus, for a conventional detector with $\delta_e=1$, the increase in $R_{NC/CC}$ due to $\overset{(-)}{\nu}_\tau$'s is a tiny 0.6%, while for the ideal detector with $\delta_e=0$, it is 4%. Since the error in the experimental measurement of the regular CC and especially NC cross sections is already of order 10%, and the uncertainty in the $\overset{(-)}{\nu}_e$ and $\overset{(-)}{\nu}_\mu$ fluxes which enter (differently) in Eqs. (4.2) and (4.3) is at least 20%, the increase in $R_{NC/CC}$ due to the $\overset{(-)}{\nu}_\tau$'s is too small to serve as a test for their presence.[20]

## V. CONCLUSIONS

In this paper we have analyzed in detail the muon trigger test proposed in Ref. 4 as a method of observing $\overset{(-)}{\nu}_\tau$ interactions, via the production and decay chain $\overset{(-)}{\nu}_\tau N\to\tau^\pm X$; $\tau^\pm\to\overset{(-)}{\nu}_\tau\mu^\pm\overset{(-)}{\nu}_\mu$. We have shown that it is the most promising and, indeed, the only feasible test for this purpose. It can be applied on an event-by-event basis, allows separate study of $\nu_\tau$- and $\bar\nu_\tau$-induced charged-current reactions, and is a specific test for $\overset{(-)}{\nu}_\tau$ which will not be confused by possible additional sequential neutrinos. When sufficiently accurate predictions for the $\overset{(-)}{\nu}_\tau$ flux become available, one will be able to use the test to determine directly whether or not $\nu_\tau$ is a sequential neutrino. To recapitulate, the dominant source of $\overset{(-)}{\nu}_\tau$ is the hadronic production of $F\bar F$ pairs, followed by the decays $F^\pm\to\tau^\pm\overset{(-)}{\nu}_\tau$. The muon trigger test consists of the requirements of (1) a single outgoing muon; (2) the standard cuts on $E_\mu$ and $E_H$; (3) substantial missing transverse momentum $(p_\perp)_{missing}>1$ GeV/$c$; and (4) distinctive azimuthal-angle correlations, as tested by the cuts $\Delta\phi_{\mu H}>90°$ and $\Delta\phi_{mH}>120°$. The $\overset{(-)}{\nu}_\tau$ signal events will also have a characteristic $y_{vis}$ distribution which vanishes as $y_{vis}\to 0$ and is peaked at large $y_{vis}$. We have demonstrated that there are no serious physics backgrounds to the $\overset{(-)}{\nu}_\tau$ signal and that, given the estimated experimental accuracy of ±0.5 GeV/$c$ in $(p_\perp)_{\text{missing}}$, the background due to imperfect measurement of $\vec{p}_H$ is manageable. In a typical experiment the total number of $\overset{(-)}{\nu}_\tau$ events obtained would be large enough to make possible a study of spectral distributions for $\nu_\tau$ and $\bar{\nu}_\tau$ charged-current reactions. Finally, we have investigated two alternative tests for $\overset{(-)}{\nu}_\tau$, one based on the double hadron shower resulting from semileptonic $\tau$ decay, and the other one based on the change in the apparent ratio of neutral-to-charged-current event rates. Our analysis indicates that neither of these two alternative tests is practical. Hopefully, however, the muon trigger test can be applied in the near future to observe, for the first time, $\nu_\tau$ and $\bar{\nu}_\tau$.

*Note added.* After the completion of this work we learned that a Columbia University–University of Illinois–NIKHEF-H (Amsterdam) collaboration, W. Y. Lee, spokesman, has recently submitted Proposal No. 625 to Fermilab for an experiment which, like the others already mentioned in the text, should be able to apply our test for $\nu_\tau$.

## ACKNOWLEDGMENTS

We would like to thank S. Mori for valuable discussions concerning neutrino fluxes in beam-dump experiments, and B. Roe, F. Taylor, J. K. Walker, and K. Winter for very helpful information about their experiments. The research of C.H.A. and J.S. was supported in part by NSF Grant Nos. PHY77-07864 and PHY79-10639 and by DOE. The research of R.S. was supported in part by DOE Contract No. EY-76-102-3072.

---

*On leave from the Institute for Theoretical Physics, State University of New York at Stony Brook, Stony Brook, New York 11973.

[1]M. L. Perl *et al.*, Phys. Rev. Lett. 35, 1489 (1975); G. Feldman *et al.*, *ibid.* 38, 117 (1977); M. L. Perl *et al.*, Phys. Lett. 63B, 466 (1976); 70B, 487 (1977) (SLAC-LBL Collaboration); A. Barbaro-Galtieri *et al.*, Phys. Rev. Lett. 39, 1058 (1977); M. Cavalli-Sforza *et al.*, *ibid.* 36, 558 (1976). For reviews see M. Perl, in *Proceedings of the 1977 International Symposium on Lepton and Photon Interactions at High Energies, Hamburg*, edited by F. Gutbrod (DESY, Hamburg, 1977); M. Perl, invited paper for the Advanced Summer Institute on New Phenomena in Lepton-Hadron Physics, Karlsruhe, 1978 (unpublished); G. J. Feldman, in *Proceedings of the 19th International Conference on High Energy Physics, Tokyo, 1978*, edited by S. Homma, M. Kawaguchi, and H. Miyazawa (Phys. Soc. of Japan, Tokyo, 1979), p. 777; G. Feldman and M. Perl, Phys. Rep. 33C, 286 (1977).

[2]W. Bacino *et al.*, Phys. Rev. Lett. 41, 13 (1978); 42, 6 (1979); 42, 749 (1979) (DELCO Collaboration); see also the reviews in Ref. 1.

[3]J. Burmester *et al.*, Phys. Lett. 68B, 297 (1977); 68B, 301 (1977); G. Alexander *et al.*, *ibid.* 73B, 99 (1978); 81B, 84 (1979) (PLUTO Collaboration); R. Brandelick *et al.*, *ibid* 70B, 125 (1977); 70B, 387 (1977); 73B, 109 (1978) (DASP Collaboration); W. Bartel *et al.*, *ibid.* 77B, 331 (1978) (DESY-Heidelberg Collaboration); for reviews, see B. Wiik and G. Wolf, DESY Report No. 78/23, 1978 (unpublished), and G. Flügge, DESY Report No. 78/42, 1978 (unpublished).

[4]C. H. Albright and R. E. Shrock, Phys. Lett. 84B, 123 (1979).

[5]M. Kobayashi and T. Maskawa, Prog. Theor. Phys. 49, 652 (1973).

[6]S. Weinberg, Phys. Rev. Lett. 19, 1264 (1967); A. Salam, in *Elementary Particle Theory: Relativistic Groups and Analyticity* (*Nobel Symposium No. 8*), edited by N. Svartholm (Almqvist and Wiksell, Stockholm, 1968), p. 367.

[7]B. Roe, F. Taylor, J. K. Walker, and K. Winter, private communications.

[8]CERN-Hamburg-Amsterdam-Rome-Moscow Collaboration, CERN Experiment WA-18, K. Winter, spokesman.

[9]Fermilab-MIT-MSU-NIU (i.e., Fermi National Accelerator Laboratory–Massachusetts Institute of Technology–Michigan State University–Northern Illinois University) Collaboration, Fermilab Experiment 594, J. K. Walker and F. E. Taylor, spokesmen.

[10]University of Michigan–Ohio State University–University of Wisconsin Collaboration, Fermilab Experiment 613, B. Roe, spokesman.

[11]F. E. Reines and C. Cowan, Phys. Rev. 113, 273 (1959); R. Carter *et al.*, *ibid.* 113, 280 (1959).

[12]G. Danby, J.-M. Gaillard, K. Goulianos, L. Lederman, N. Mistry, M. Schwartz, and J. Steinberger, Phys. Rev. Lett. 9, 36 (1962).

[13]M. Perl, G. Feldman, Ref. 1; B. Wiik and G. Wolf, Ref. 3; G. Flügge, Ref. 3.

[14]Of course one can only define the gauge group eigenstates $\nu_i$ and the corresponding mass eigenstates $L_i$, where $i = e, \mu, \tau, \ldots$, to coincide if the $m(L_i^0)$ are all equal [for example, if, as one expects, $m(L_i^0) = 0$ for all $i$]. What is meant by "$m(\nu_\tau) < 0.25$ GeV" is really "$m(L_\tau^0) \lesssim 0.25$ GeV."

[15]A. M. Cnops *et al.*, Phys. Rev. Lett. 40, 145 (1978). This (BNL-Columbia-Fermilab) experiment obtained the upper bound $g_{\tau\nu_\tau} < 0.025 g_{\mu\nu_\mu}$. Together with the lower bound $g_{\tau\nu_\tau} > 0.35 g_{\mu\nu_\mu}$ from the DELCO experiment, Ref. 2, this rules out the possibility that $\nu_\tau = \overset{(-)}{\nu}_\mu$.

[16]S. L. Glashow, J. Illiopoulos, and L. Maiani, Phys. Rev. D 2, 1285 (1970).

[17]For recent reviews of the experimental status of the standard Weinberg-Salam $SU(2)_L \times U(1)$ gauge theory, see, e.g., C. Baltay and S. Weinberg, in *Proceedings of the 19th International Conference on High Energy Physics, Tokyo, 1978* (Ref. 1).

[18]S. L. Glashow and S. Weinberg, Phys. Rev. D 15, 1458 (1977); E. A. Paschos, *ibid.* 15, 1966 (1977).

[19]B. W. Lee and R. E. Shrock, Phys. Rev. D 16, 1444

(1977). See also T. P. Cheng and L. F. Li, Phys. Rev. Lett. 38, 381 (1977); Phys. Rev. D 16, 1425 (1977); S. Treiman, F. Wilczek, and A. Zee, *ibid.* 16, 152 (1977); J. Bjorken, K. Lane, and S. Weinberg, *ibid.* 16, 1474 (1977); and W. Marciano and A. Sanda, Phys. Lett. 67B, 303 (1977).

[20]V. Barger and R. Phillips, Phys. Lett. 74B, 393 (1978). In this reference an analog to the $R_{NC/CC}$ test discussed in the present paper (in Sec. II) was proposed. The Barger-Phillips test differs from our $R_{NC/CC}$ test in that it assumes that charmed hadrons do not decay to $\tau^{\pm}\overset{(-)}{\nu}_\tau$, so that the dominant source of $\overset{(-)}{\nu}_\tau$ is claimed to be the hadronic production and (semi)leptonic decays of heavy $b$- and $t$-flavored hadrons. No estimates were given by these authors for the absolute $\overset{(-)}{\nu}_\tau$ flux or for the ratio $N(\overset{(-)}{\nu}_\tau)/N(\overset{(-)}{\nu}_l)$, where $l = e$ of $\mu$. However, from our analysis of the $\overset{(-)}{\nu}_\tau$ flux and of the $R_{NC/CC}$ test, in Sec. II and IV, respectively, it is clear that the Barger-Phillips test is hopeless; the $\overset{(-)}{\nu}_\tau$ flux from the decays of $b$-flavored (and, *a fortiori*, from $t$-flavored) hadrons is too small by a factor of $\sim 10^3$ for their test to work.

[21]This estimate has also been used by F. Sciulli, in *Neutrinos-78*, edited by E. Fowler (Purdue University, West Lafayette, Indiana, 1978).

[22]P. Alibran *et al.*, Phys. Lett. 74B, 134 (1978); T. Hansl *et al.*, *ibid.* 74B, 139 (1978); P. Bosetti *et al.*, *ibid.* 74B, 143 (1978); M. Shaevitz, in *Particle Searches and Discoveries-1978* (AIP, New York, 1978). See also the review by H. Wachsmuth, in *Proceedings of the Topical Conference on Neutrino Physics at Accelerators, Oxford, 1978*, edited by D. Perkins (Rutherford Laboratory, Chilton, Didcot, Oxfordshire, England, 1978).

[23]R. E. Shrock and L.-L. Wang, Phys. Rev. Lett. 41, 1692 (1978).

[24]R. E. Shrock, S. B. Treiman, and L.-L. Wang, *ibid.* 42, 1589 (1979); R. E. Shrock and L.-L. Wang (unpublished).

[25]See, e.g., V. Novikov *et al.*, Phys. Rev. Lett. 38, 627 (1977); 38, 791(E) (1977); and a discussion of the analogous pseudoscalar decay constant for $b$-flavored mesons in R. Cahn and S. D. Ellis, Phys. Rev. D 16, 1484 (1977).

[26]See, for example, review by E. Lohrmann, in *Proceedings of the 1977 International Symposium on Lepton and Photon Interactions at High Energies, Hamburg* (Ref. 1) and references therein.

[27]R. Brandelik *et al.* (DASP Collaboration), Phys. Lett. 70B, 132 (1977); 80B, 412 (1979); D. Luke, in *Particles and Fields—1977*, proceedings of the Meeting of the APS Division of Particles and Fields, Argonne, edited by P. A. Schreiner, G. H. Thomas, and A. B. Wicklund (AIP, New York, 1978).

[28]The role of the $F$ as a source of $\overset{(-)}{\nu}_\tau$'s was discussed, and the possibility of using the double-shower test for $\overset{(-)}{\nu}_\tau$ was suggested, by F. Sciulli, Ref. 21.

[29]See, e.g., T. Gaisser and F. Halzen, Phys. Rev. D 14, 3153 (1976); M. Goldhaber and L.-L. Wang, *ibid.* 18, 2364 (1978). For specific model calculations which yield somewhat larger and smaller values of this ratio, respectively, see F. Halzen and S. Matsuda, Phys. Rev. D 17, 1344 (1978); and B. Combridge, Nucl. Phys. B151, 429 (1979).

[30]S. D. Drell and T.-M. Yan, Phys. Rev. Lett. 25, 316 (1970); Ann. Phys. (N.Y.) 66, 578 (1971).

[31]For a review, see L. Lederman, in *Proceedings of the 19th International Conference on High Energy Physics, Tokyo, 1978* (Ref. 1).

[32]R. Bhattacharya, J. Smith, and A. Soni, Phys. Rev. D 13, 2150 (1976). Bethe-Heitler production of $\tau^+\tau^-$ pairs in $pN$ collisions has an even smaller cross section than the Drell-Yan process; see J. Smith, A. Soni, and J. Vermaseren, Phys. Rev. D 15, 648 (1977).

[33]See, for example, R. Stefanski and H. White, Fermilab Report No. FN-292, 1976 (unpublished).

[34]M. Bourquin and J.-M. Gaillard, Phys. Lett. 58B, 191 (1975); Nucl. Phys. B114, 334 (1976); I. Hinchliffe and C. H. Llewellyn Smith, *ibid.* B114, 45 (1976). See also J. Bourotte, thesis, Universeté de Paris-Sud, 1978 (unpublished).

[35]S. Mori, Fermilab Reports No. TM-774 and No. TM-848, 1979 (unpublished). We have rescaled Mori's flux results so all the curves refer to a copper (rather than aluminum) dump 250 m upstream of a suitable detector subtending an angle of 0–2 mrad with respect to the primary-proton-beam direction and assumed on $A$ dependence for $D$ and $F$ production (rather than $A^{2/3}$).

[36]B. Roe, University of Michigan Research Note, 1978 (unpublished); see also B. Roe, spokesman, Fermilab Proposal 613, Ref. 10.

[37]The operational definition $(\vec{p}_H)_{\exp} \equiv E_H \hat{p}_H$ is used instead of the exact expression $(\vec{p}_H)_{\text{exact}} = (E_H{}^2 - W^2)^{1/2}\, \hat{p}_H$, where $W$ denotes the hadronic invariant mass, because $W$ is not measured directly and cannot be reconstructed as in regular neutrino reactions via the relation $W^2 = 2m_N E y(1-x) + m_N{}^2$; this, in turn, is a consequence of the fact that the $x$ value of the primary $\overset{(-)}{\nu}_\tau N \to \tau^{\pm} X$ scattering cannot be determined. However, the operation definition is an extremely good approximation; for example, with the typical values $E = 50$ GeV, $x = 0.3$, $y = 0.5$, $(\vec{p}_H)_{\text{exact}} = 0.99 (\vec{p}_H)_{\exp}$.

[38]C. H. Albright and C. Jarlskog, Nucl. Phys. B84, 467 (1975); C. H. Albright, C. Jarlskog, and L. Wolfenstein, *ibid.* B84, 493 (1975). A special case of these calculations was later repeated, and the effect on the $y_{\text{vis}}$ distribution noted, by J. Losecco, Phys. Rev. D 18, 1439 (1978). However, Losecco neglected the effect of the heavy-lepton mass (which had been properly included in the 1975 papers cited above).

[39]J. Smith, in *Neutrinos-78*, edited by E. Fowler (Purdue University, Lafayette, 1978); G. Kane, J. Smith, and J. Vermaseren, Phys. Rev. D 19, 1978 (1979); T. Hansl *et al.*, Phys. Lett. 77B, 114 (1978); Nucl. Phys. B142, 381 (1978); A. K. Mann and K. Tittel, in *Proceedings of the 19th International Conference on High Energy Physics, Tokyo* (Ref. 1).

[40]C. H. Albright and J. Smith, Phys. Lett. 77B, 94 (1978).

[41]There is a cosmological bound on the number, $n$, of neutrinos, and thus of lepton doublets in the standard model, based on primordial helium production. Depending on which measured values and corrections were taken, one obtains $n \lesssim 7$ [cf. G. Steigman, D. Schramm, and J. Gunn, Phys. Lett. 66B, 202 (1977)] or more recently, an even smaller value of $n$ [cf. J. Yang, D. Schramm, G. Steigman, and R. Rood, Astrophys. J. 227, 697 (1979). There is, however, a large scatter in the measured values of helium abundance and commensurately large uncertainties in the inferred bounds. We thank J. Peebles for dis-

cussions on this point.

[42]C. Berger *et al.* (PLUTO detector), Phys. Lett. 81B, 410 (1979); D. Barber *et al.* (MARK J detector), Phys. Rev. Lett. 42, 1113 (1979); preliminary results from the TASSO detector are quoted by R. Devenish, in the informal Proceedings of the Caltech Workshop on High Energy Physics, 1979 (unpublished).

[43]For an example of such an obsolete theory, featuring new $\nu_l L^-$ couplings, see B. W. Lee and S. Weinberg, Phys. Rev. Lett. 38, 1237 (1977); B. W. Lee and R. E. Shrock, Phys. Rev. D 17, 2410 (1978). For another obsolete model [based on the same gauge group, SU(3) $\times$U (1)] featuring a $\nu_l L^0$ coupling, see P. Langacker and G. Segrè, Phys. Rev. Lett. 39, 259 (1977).

[44]M. Holder *et al.*, Phys. Lett. 74B, 277 (1978).

[45]C. H. Albright, J. Smith, and J. Vermaseren, Phys. Rev. Lett. 38, 1187 (1977); Phys. Rev. D 16, 3182, 3204 (1977). For a general review, of mechanisms of trimuon production, see J. Smith, in *Neutrinos—78* (Ref. 39).

[46]T. Hansl *et al.*, Phys. Lett. 77B, 114 (1978); Nucl. Phys. B142, 381 (1978).

[47]A. M. Cnops *et al.* (Ref. 15). For assumptions concerning the chirality of the production vertex and the electron branching ratio, see Ref. 15.

[48]H. Ballagh, *et al.*, Phys. Lett. 79B, 320 (1978).

[49]C. H. Albright, Phys. Rev. Lett. 28, 1150 (1972); Phys. Rev. D 7, 63 (1973); 12, 1319 (1975); L.-N. Chang, E. Derman, and J. Ng, Phys. Rev. Lett. 35, 6 (1975); Phys. Rev. D 12, 3539 (1975); A. Pais and S. B. Treiman, Phys. Rev. Lett. 35, 1206 (1975); Phys. Rev. D 14, 293 (1976).

[50]For recent reviews of dilepton production in neutrino reactions, see B. Barish and D. Cline, in *Proceedings of the 1977 International Symposium on Lepton and Photon Interactions at High Energies, Hamburg* (Ref. 1); and C. Baltay and K. Tittel, in *Proceedings of the 19th International Conference on High Energy Physics, Tokyo, 1978* (Ref. 1).

[51]M. Hibbs *et al.*, Bull. Am. Phys. Soc. 24, 23 (1979).

[52]L. Fluri *et al.*, Bull. Am. Phys. Soc. 24, 24 (1979); M. Sokoloff *et al.*, *ibid.* 24, 655 (1979).

[53]C. H. Albright and C. Jarlskog (Ref. 38).

[54]R. E. Shrock, Phys. Rev. Lett. 40, 1688 (1978).

[55]B. W. Lee and S. Weinberg, Phys. Rev. Lett. 39, 165 (1977).

[56]We follow the convention used by expermentalists of writing this coupling-constant bound as a bound on $g_{\tau\nu_\tau}{}^2$. However, it is really a bound on this squared coupling multiplied by the appropriate sum of squares of the couplings to leptons and quarks of the gauge boson which mediates the $\tau\nu_\tau$ transition. That is, the bound should be written as

$$g_{V\tau\nu_\tau}{}^2(g_{Ve\nu_e}{}^2+g_{V\mu\nu_\mu}{}^2+3g_{Vd_Cu}{}^2)\gtrsim 0.12\,(5g_{Wl\nu_l}{}^4)\,,$$

where $V$ denotes the gauge boson which mediates the $\tau\nu_\tau$ transition, $d_C \equiv V_{ud}\,d+V_{us}s$, in the notation of Ref. 24, $W$ denotes the usual charged vector boson, and $g_{Wl\nu_l}$ is the coupling of $W$ to $l_{\nu l}$, $l=e$ or $\mu$. Using the fact that $B(\tau\to\nu_\tau e\bar{\nu}_e)\simeq B(\tau\to\nu_\tau\mu\bar{\nu}_\mu)\simeq 0.2$, we can rewrite this bound as $g_{V\tau\nu_\tau}{}^2 g_{Vl\nu_l}{}^2>0.12g_{Wl\nu_l}{}^4$. Thus, this complication does not affect our use of the bound, since the product of couplings which occurs in $\tau$ decay and hence on the left-hand side of the above inequality is the same as the one which occurs in the cross section for $\overset{(-)}{\nu}_\tau N\to\tau^\pm X$ where the inferred result $g_{Vl\nu_l}{}^2\simeq g_{Vd_Cu}{}^2$ has been used).

[57]B. W. Lee and R. E. Shrock (Ref. 19). The constraints discussed in this paper are general, although they were applied to a special version of the Kobayashi-Maskawa model in which $m(L_3^0)>m(L_3^-)$ and $L_3$ was not assumed necessarily to be the $\tau$.